Quantum Fluctuation Theorems for Arbitrary Environments: Adiabatic and Nonadiabatic Entropy Production

Gonzalo Manzano,[1,2,*] Jordan M. Horowitz,[3] and Juan M. R. Parrondo[1]

[1]*Departamento de Física Atómica, Molecular y Nuclear and GISC, Universidad Complutense Madrid, 28040 Madrid, Spain*

[2]*IFISC (UIB-CSIC), Instituto de Física Interdisciplinar y Sistemas Complejos, UIB Campus, E-07122 Palma de Mallorca, Spain*

[3]*Physics of Living Systems Group, Department of Physics, Massachusetts Institute of Technology, 400 Technology Square, Cambridge, Massachusetts 02139, USA*

(Received 25 October 2017; revised manuscript received 30 May 2018; published 6 August 2018)

We analyze the production of entropy along nonequilibrium processes in quantum systems coupled to generic environments. First, we show that the entropy production due to final measurements and the loss of correlations obeys a fluctuation theorem in detailed and integral forms. Second, we discuss the decomposition of the entropy production into two positive contributions, adiabatic and nonadiabatic, based on the existence of invariant states of the local dynamics. Fluctuation theorems for both contributions hold only for evolutions verifying a specific condition of quantum origin. We illustrate our results with three relevant examples of quantum thermodynamic processes far from equilibrium.

DOI: 10.1103/PhysRevX.8.031037

Subject Areas: Quantum Physics, Quantum Information, Statistical Physics

I. INTRODUCTION

Classical thermodynamics and statistical mechanics provide a systematic approach to the phenomenology of a system immersed in a large environment. Within these frameworks, two complementary strategies are employed. The first is to explicitly model the environment—often an equilibrium thermal reservoir—to obtain an effective reduced dynamics for the system alone, which then can be analyzed. The second is to derive fundamental constraints in the form of inequalities using the second law of thermodynamics and magnitudes like entropy, entropy production, and free energy. The recent introduction of an entropy for stochastic trajectories [1] allows one to refine these inequalities with exact equalities for arbitrary nonequilibrium processes, results generically known as fluctuation theorems (FT's) [2,3].

These two strategies have also been successfully applied to quantum systems. Open quantum system dynamics—the determination and analysis of the system's reduced dynamics—is a well-developed and active field [4,5]. Complementing this approach, a variety of quantum FT's have been derived [6–11] to assess the statistics of the relevant quantities. Different proposals to obtain these statistics in the laboratory have been reported, using techniques related to quantum tomography [12–17], and some of them have already been used to carry out experimental verifications of FT's [18,19]. However, most of the research on quantum FT's is only valid for equilibrium reservoirs with a focus on the energy exchange between the system and the environment in the form of heat and work. By contrast, classical FT's have been formulated more generally for generic Markov systems [20–24] using the entropy production instead of heat and work, which are only meaningful in physical situations where a system exchanges energy with equilibrium reservoirs.

In light of the success of classical FT's, it is desirable to obtain complementary FT's for generic quantum dynamics [25–35]. They could be of particular relevance since quantum mechanics allows for a richer phenomenology in finite baths [36–38], as well as novel and interesting nonthermal environments such as coherent [39,40], correlated [41], or squeezed [42–45] reservoirs. Such environments induce an interesting phenomenology that goes beyond the thermodynamics of thermal equilibrium reservoirs, such as heat engines that outperform Carnot efficiency [46] and may exhibit new regimes of operation [45,47] or tighter bounds on Landauer's principle [48,49].

The task of deriving FT's for generic quantum dynamics also implies a more detailed characterization of

*gmanzano@ucm.es

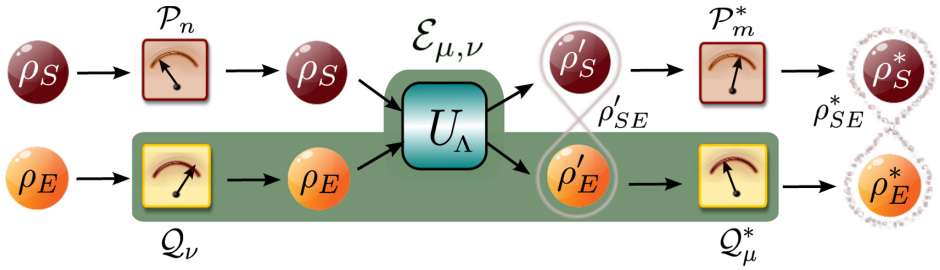

FIG. 1. Schematic picture of the forward process presented in the main text. The system and environment start from an uncorrelated state $\rho_S \otimes \rho_E$. A local measurement of observables with projectors $\{\mathcal{P}_n, \mathcal{Q}_\nu\}$ is carried out, which does not alter the density matrix in the average evolution but selects a pure state $|\psi_n\rangle \otimes |\phi_\nu\rangle$ at the trajectory level. The system and environment then interact with each other according to the unitary evolution U_Λ, ending in an entangled state ρ'_{SE}. Finally, we measure again, now using projectors $\{\mathcal{P}^*_m, \mathcal{Q}^*_\mu.\}$. In the last measurement, quantum correlations in state ρ'_{SE} are erased, while the final state ρ^*_{SE} may still have, in general, nonzero classical correlations. The reduced evolution of the system conditioned to the measurement in the environment is described through the quantum operation $\mathcal{E}_{\mu\nu}$ (shaded area).

entropy production in nonequilibrium quantum contexts, a problem that has attracted a growing interest in recent years [8,30,31,33,50–57]. In Ref. [33], we derived a FT for a class of completely positive trace-preserving (CPTP) quantum maps, which model a variety of quantum processes. Through this analysis, we identified a quantity that coincides with the entropy production for thermalization processes and resembles the nonadiabatic entropy production introduced in the classical context [21–23]. The purpose of this paper is to clarify and extend those results, considering together the system and its surroundings. By tracing over the environment, we can then recover the quantum map for the reduced system dynamics. This setup allows us to unveil the origin of entropy production in arbitrary processes from coarse graining and derive corresponding FT's. We also split the entropy production into an adiabatic and a nonadiabatic contribution, exactly as in classical stochastic thermodynamics. However, contrary to what happens in classical systems, the split is not always possible. A condition, derived in Ref. [33], is necessary. We explore the similarities and differences between classical and quantum FT's in concrete examples.

The paper is organized as follows. In Sec. II, we introduce a thermodynamic process for a generic bipartite system that models a system and its environment. In this section, we define the entropy production along the process and the concomitant reduced system dynamics. We develop a FT for this entropy production in Sec. III using a time-reversed or backward thermodynamic process. In Sec. IV, FT's for the adiabatic and nonadiabatic entropy production are derived. Our results are also extended both to the case of concatenations of CPTP maps and multipartite environments. This is applied to the specific case of quantum trajectories unraveled from Lindblad master equations in Sec. V. Finally, relevant examples to illustrate our results are given in Sec. VI, and we conclude in Sec. VII with some final remarks.

II. QUANTUM OPERATIONS AND ENTROPY PRODUCTION

Throughout the paper, we consider an isolated quantum system composed of two parts, system and environment (or ancilla), with Hilbert space $\mathcal{H} \equiv \mathcal{H}_S \otimes \mathcal{H}_E$, where $\mathcal{H}_S$ and $\mathcal{H}_E$ are the local Hilbert spaces of the system and the environment, respectively. We focus our attention on the entropy production along the generic process depicted in Fig. 1, consisting of initial and final local projective measurements that bracket a unitary evolution. The outcomes of the measurements constitute a quantum trajectory, which plays a crucial role in the formulation of FT's.

A. The (forward) process

The process begins with the global system in an uncorrelated product state $\rho_{SE} = \rho_S \otimes \rho_E$. The spectral decomposition of the local states reads

$$\rho_S = \sum_n p_n \mathcal{P}_n, \qquad \rho_E = \sum_\nu q_\nu \mathcal{Q}_\nu, \tag{1}$$

where p_n and q_ν are the eigenvalues, and $\{\mathcal{P}_n\}$ and $\{\mathcal{Q}_\nu\}$ are orthogonal projectors onto their respective eigensubpaces (for simplicity, we assume they are rank-1 projectors).

At $t = 0$, an initial projective measurement on the system and environment is performed using the eigenprojectors in Eq. (1), and outcomes n and ν are obtained. This measurement projects the system and environment onto pure states $|\psi_n\rangle\langle\psi_n|_S \equiv \mathcal{P}_n$ and $|\phi_\nu\rangle\langle\phi_\nu|_E \equiv \mathcal{Q}_\nu$, without modifying the average or unconditional state of the global system ($[\mathcal{P}_n\mathcal{Q}_\nu, \rho_{SE}] = 0$).

Subsequently, we evolve the compound system during the time interval $[0, \tau]$. The corresponding unitary operator U_Λ is generated by the Hamiltonian $H(t) = H(\lambda_t)$, which depends on time through an external parameter λ_t that we vary according to a prescribed protocol $\Lambda = \{\lambda_t : 0 \le t \le \tau\}$:

$$U_\Lambda \equiv \mathcal{T}_+ \exp\left(-\frac{i}{\hbar}\int_0^\tau dt\, H(\lambda_t)\right), \tag{2}$$

where $\mathcal{T}_+$ denotes the time-ordering operator. As a result, the compound system at time $t=\tau$ is described by the new density matrix

$$\rho'_{SE} = U_\Lambda(\rho_S \otimes \rho_E)U_\Lambda^\dagger, \tag{3}$$

which, in general, contains classical and quantum correlations. The reduced (or local) states of the system and the environment can be obtained by partial tracing: $\rho'_S = \mathrm{Tr}_E[\rho'_{SE}]$ and $\rho'_E = \mathrm{Tr}_S[\rho'_{SE}]$.

To complete the process, a second local projective measurement is performed at time $t=\tau$ on both the system and the environment. The measurement operators are arbitrary (rank-1) orthogonal projectors, denoted as $\{\mathcal{P}^*_m\}$ and $\{\mathcal{Q}^*_\mu\}$. Unlike in the first measurement, in this case, the average global state is disturbed, transforming into

$$\begin{aligned}\rho^*_{SE} &= \sum_{m,\mu}(\mathcal{P}^*_m \otimes \mathcal{Q}^*_\mu)\rho'_{SE}(\mathcal{P}^*_m \otimes \mathcal{Q}^*_\mu)\\ &= \sum_{m,\mu}\varrho^*_{m\mu}(\mathcal{P}^*_m \otimes \mathcal{Q}^*_\mu).\end{aligned} \tag{4}$$

Notice also that this is not a product state: The final local measurement does not eliminate the classical correlations contained in ρ^*_{SE} [58]. However, the measurement collapses the local states of the system and environment into pure states $|\psi^*_m\rangle\langle\psi^*_m|_S \equiv \mathcal{P}^*_m$ and $|\phi^*_\mu\rangle\langle\phi^*_\mu|_E \equiv \mathcal{Q}^*_\mu$. Thus, the spectral decomposition of the reduced states after the final measurement is

$$\rho^*_S \equiv \mathrm{Tr}_E(\rho^*_{SE}) = \sum_m p^*_m \mathcal{P}^*_m, \tag{5}$$

$$\rho^*_E \equiv \mathrm{Tr}_S(\rho^*_{SE}) = \sum_\mu q^*_\mu \mathcal{Q}^*_\mu, \tag{6}$$

where $p^*_m = \sum_\mu \varrho^*_{m\mu}$ and $q^*_\mu = \sum_m \varrho^*_{m\mu}$ are the corresponding classical marginal distributions.

B. Reduced dynamics: Maps and operations

The global manipulation described above induces a reduced dynamics on the system alone. The shaded area in Fig. 1 can be considered as an effective transformation of the state of the system, $\rho_S \to \rho'_S$, described by the action of a quantum CPTP map $\mathcal{E}$ that admits a Kraus representation [59]

$$\rho'_S = \mathcal{E}(\rho_S) = \sum_{\mu,\nu} M_{\mu\nu}\rho_S M^\dagger_{\mu\nu}, \tag{7}$$

with a set of Kraus operators $M_{\mu\nu}$ satisfying $\sum_{\mu,\nu} M^\dagger_{\mu\nu}M_{\mu\nu} = \mathbb{I}$.

There exist many Kraus representations $\{M_{\mu\nu}\}$ that reproduce the reduced dynamics on the system. We choose

$$M_{\mu\nu} = \sqrt{q_\nu}\langle\phi^*_\mu|_E U_\Lambda|\phi_\nu\rangle_E. \tag{8}$$

This specific representation retains all the details of the evolution of the environment, unequivocally relating each Kraus operator $M_{\mu\nu}$ with a transition $|\phi_\nu\rangle_E \to |\phi^*_\mu\rangle_E$ in the environment. This is a key point in order to characterize the thermodynamics of the process at the trajectory level, as we will see shortly. Let us finally define the quantum operation:

$$\mathcal{E}_{\mu\nu}(\rho_S) = M_{\mu\nu}\rho_S M^\dagger_{\mu\nu}, \tag{9}$$

which describes the conditioned evolution of the system when the environment starts in the pure state $|\phi_\nu\rangle_E$ and ends in the state $|\phi^*_\mu\rangle_E$ after measurement [60].

C. Average entropy production

We now discuss the entropy change along the process. We analyze here the von Neumann entropy, $S(\rho) = -\mathrm{Tr}[\rho\ln\rho]$, of the global system. Recall that the von Neumann entropy coincides with the thermodynamic entropy for equilibrium states (setting the Boltzmann constant $k=1$). For nonequilibrium states, there are some situations where the von Neumann entropy can still be interpreted as a thermodynamic entropy [61]. However, in this paper, we refrain from identifying $S(\rho)$ with a thermodynamic entropy and refer to it simply as the entropy or the quantum entropy of state ρ.

Along the process described above, the quantum entropy of the global system changes as

$$\Delta_{\mathrm{i}}S_{\mathrm{inc}} \equiv S(\rho^*_{SE}) - S(\rho_{SE}). \tag{10}$$

This quantity is the quantum entropy production along the process. We refer to $\Delta_{\mathrm{i}}S_{\mathrm{inc}}$ as the inclusive entropy production to distinguish it from the entropy production when the system and the environment are separated at the end of the process and the final classical correlations are lost (see below). The inclusive entropy production is always non-negative; this is because von Neumann entropy cannot decrease in a projective measurement, and it stays constant along any unitary evolution, i.e., $S(\rho_{SE}) = S(\rho'_{SE}) \le S(\rho^*_{SE})$. Notice also that $S(\rho)$ equals the classical Shannon entropy of the probability distribution of pure states in the eigenbasis of ρ. In particular, we have

$$S(\rho_{SE}) = -\sum_{n,\nu} p_n q_\nu \ln(p_n q_\nu), \tag{11}$$

$$S(\rho^*_{SE}) = -\sum_{m,\mu} \varrho^*_{m\mu}\ln\varrho^*_{m\mu}. \tag{12}$$

To express the entropy of the global state in terms of local entropies and correlations, one can use the mutual information. For an arbitrary state σ_{SE} with reduced states σ_S and σ_E, the mutual information is defined as

$$\begin{aligned}\mathcal{I}(\sigma_{SE}) &\equiv S(\sigma_S) + S(\sigma_E) - S(\sigma_{SE}) \\ &= S(\sigma_{SE}||\sigma_S \otimes \sigma_E). \end{aligned} \tag{13}$$

Here, we have introduced the quantum relative entropy, $S(\rho||\sigma) \equiv \mathrm{Tr}[\rho(\ln\rho - \ln\sigma)]$, a nonsymmetric and non-negative measure of the distinguishability between states ρ and σ, which vanishes if and only if $\rho = \sigma$ [62]. This property implies that mutual information becomes zero only for product (uncorrelated) states $\sigma_{SE} = \sigma_S \otimes \sigma_E$. Using mutual information, the inclusive entropy production can be rewritten as

$$\begin{aligned}\Delta_{\mathrm{i}} S_{\mathrm{inc}} &= S(\rho_S^*) - S(\rho_S) + S(\rho_E^*) - S(\rho_E) - \mathcal{I}(\rho_{SE}^*) \\ &= S(\rho_S^*) - S(\rho_S') + S(\rho_E^*) - S(\rho_E') \\ &\quad + \mathcal{I}(\rho_{SE}') - \mathcal{I}(\rho_{SE}^*) \geq 0, \end{aligned} \tag{14}$$

where we have taken into account that the initial state is uncorrelated and, therefore, $\mathcal{I}(\rho_{SE}) = 0$. The second equality shows that there are two sources of entropy production. The first one is the measurement disturbance of the final local states $\rho_S' \to \rho_S^*$ and $\rho_E' \to \rho_E^*$, which can be avoided only by measuring in the eigenbasis of the reduced states ρ_S' and ρ_E'. The second source, captured by the term $\mathcal{I}(\rho_{SE}') - \mathcal{I}(\rho_{SE}^*) \geq 0$, is the erasure of quantum correlations in the state ρ_{SE}'. This is due to the local character of the measurements, which is zero only if the global interaction U_Λ does not generate quantum correlations [63,64].

In most situations, the classical correlations remaining after the final measurement are irreversibly lost, with an entropic cost equal to the mutual information $\mathcal{I}(\rho_{SE}^*)$. This is the case if we separate the system and environment after the process and all subsequent manipulations are local and do not incorporate any feedback based on the outcomes of the final measurements. The entropy production in those situations is

$$\Delta_{\mathrm{i}} S \equiv S(\rho_S^*) - S(\rho_S) + S(\rho_E^*) - S(\rho_E). \tag{15}$$

We refer to $\Delta_{\mathrm{i}} S$ as the noninclusive entropy production or simply entropy production. The positivity of the noninclusive entropy production in Eq. (15) has already been identified with the second law [48] and the existence of a thermodynamic arrow of time [65,66]. Notice that $\Delta_{\mathrm{i}} S \geq \Delta_{\mathrm{i}} S_{\mathrm{inc}} \geq 0$ since the mutual information $\mathcal{I}(\rho_{SE}^*)$ is always non-negative.

The differences between inclusive and noninclusive entropy production will be illustrated in a specific example in Sec. VI A.

III. BACKWARD PROCESS AND FLUCTUATION THEOREM FOR THE ENTROPY PRODUCTION

A. Forward and backward trajectories

We now extend the previous analysis to stochastic entropy changes at the level of individual quantum trajectories. A trajectory γ of the process introduced in the previous section (hereafter, we call it the forward process) is simply given by the outcome of the four measurements, i.e., $\gamma = \{n, \nu, \mu, m\}$. This trajectory corresponds to the following transition between pure states:

$$|\psi_n\rangle_S \otimes |\phi_\nu\rangle_E \to |\psi_m^*\rangle_S \otimes |\phi_\mu^*\rangle_E. \tag{16}$$

Notice that, in virtue of our choice of the Kraus representation for the reduced dynamics [Eq. (8)], a trajectory γ is also a trajectory of the reduced dynamics, where the pair (ν, μ) now indicates the Kraus operation affecting the system instead of the initial and final states of the environment (which is otherwise hidden in the reduced dynamics). The probability to observe trajectory γ is given by

$$P(\gamma) = p_n q_\nu \mathrm{Tr}[(\mathcal{P}_m^* \otimes \mathcal{Q}_\mu^*) U_\Lambda (\mathcal{P}_n \otimes \mathcal{Q}_\nu) U_\Lambda^\dagger]. \tag{17}$$

To introduce the backward process, we make use of the antiunitary time-reversal operator in quantum mechanics, Θ, satisfying $\Theta\Theta^\dagger = \Theta^\dagger\Theta = \mathbb{I}$ and $\Theta i = -i\Theta$. This operator changes the sign of odd variables under time reversal, like linear and angular momenta or magnetic fields [6,67]. We consider the separate time-reversal operators for the system, Θ_S, and environment, Θ_E, as well as the one for the total bipartite system, $\Theta = \Theta_S \otimes \Theta_E$.

The backward process is defined as follows. We start with a generic initial state of the form

$$\tilde{\rho}_{SE} = \sum_{m,\mu} \tilde{\varrho}_{m\mu} \Theta_S \mathcal{P}_m^* \Theta_S^\dagger \otimes \Theta_E \mathcal{Q}_\mu^* \Theta_E^\dagger. \tag{18}$$

As in the forward process, the first step at time $t = 0$ is a local measurement of the family of projectors $\{\Theta_S \mathcal{P}_m^* \Theta_S^\dagger, \Theta_E \mathcal{Q}_\mu^* \Theta_E^\dagger\}$. According to Eq. (18), the outcomes m and μ are obtained with probability $\tilde{\varrho}_{m\mu}$. We then let the global system evolve under the Hamiltonian $\Theta H(\lambda_t)\Theta^\dagger$ inverting the time-dependent protocol as $\tilde{\Lambda} \equiv \{\tilde{\lambda}_t | 0 \leq t \leq \tau\}$ with $\tilde{\lambda}_t = \lambda_{\tau - t}$. This evolution is given by the unitary transformation

$$U_{\tilde{\Lambda}} \equiv \mathcal{T}_+ \exp\left(-\frac{i}{\hbar}\int_0^\tau dt\, \Theta H(\tilde{\lambda}_t)\Theta^\dagger\right). \tag{19}$$

Finally, at time $t = \tau$, we perform new local measurements on the system and environment using projectors $\{\Theta_S \mathcal{P}_n \Theta_S^\dagger, \Theta_E \mathcal{Q}_\nu \Theta_E^\dagger\}$. The outcome induces a quantum jump

$$\Theta(|\psi_m^*\rangle_S \otimes |\phi_\mu^*\rangle_E) \to \Theta(|\psi_n\rangle_S \otimes |\phi_\nu\rangle_E), \tag{20}$$

and the corresponding backward trajectory $\tilde{\gamma} = \{m, \mu, \nu, n\}$ occurs with probability

$$\tilde{P}(\tilde{\gamma}) = \tilde{\varrho}_{m\mu} \mathrm{Tr}[\Theta(\mathcal{P}_n \otimes \mathcal{Q}_\nu)\Theta^\dagger U_{\tilde{\Lambda}} \Theta(\mathcal{P}_m^* \otimes \mathcal{Q}_\mu^*)\Theta^\dagger U_{\tilde{\Lambda}}^\dagger]. \tag{21}$$

B. Fluctuation theorem

The unitary transformations corresponding to the forward and the backward process satisfy the so-called microreversibility principle for nonautonomous systems [6,68]:

$$\Theta^\dagger U_{\tilde{\Lambda}} \Theta = U_\Lambda^{-1} = U_\Lambda^\dagger. \tag{22}$$

This is the key property that relates the probabilities of trajectories γ and $\tilde{\gamma}$ in a quantum FT. By comparing the probabilities (17) and (21), using microreversibility (22) and the cyclic property of the trace, we immediately get

$$\Delta_\mathrm{i} s_\gamma \equiv \ln \frac{P(\gamma)}{\tilde{P}(\tilde{\gamma})} = \ln \frac{p_n q_\nu}{\tilde{\varrho}_{m,\mu}} = \sigma_{nm}^S + \sigma_{\nu\mu}^E - \tilde{I}_{m\mu}, \tag{23}$$

where we have defined the quantities

$$\sigma_{nm}^S = \ln p_n - \ln \tilde{p}_m, \qquad \sigma_{\mu\nu}^E = \ln q_\nu - \ln \tilde{q}_\mu, \tag{24}$$

$$\tilde{I}_{m,\mu} = \ln \tilde{\varrho}_{m,\mu} - \ln \tilde{p}_m \tilde{q}_\mu. \tag{25}$$

The terms in Eq. (24) are related to entropy changes per trajectory in the system and the environment, whereas $\tilde{I}_{m,\mu}$ in Eq. (25) corresponds to the stochastic version of the mutual information [25,69] in the initial state of the backward process (18). From the detailed FT in Eq. (23), we immediately have the integral version

$$\langle e^{-\Delta_\mathrm{i} s_\gamma} \rangle = \sum_\gamma P(\gamma) e^{-\Delta_\mathrm{i} s_\gamma} = \sum_\gamma \tilde{P}(\tilde{\gamma}) = 1, \tag{26}$$

and, using Jensen's inequality $\langle e^x \rangle \geq e^{\langle x \rangle}$, one obtains a second-law-like expression $\langle \Delta_\mathrm{i} s_\gamma \rangle = \langle \sigma^S \rangle + \langle \sigma^E \rangle - \langle \tilde{I} \rangle \geq 0$.

The interpretation of $\Delta_\mathrm{i} s_\gamma$ depends on the choice of $\tilde{\rho}_{SE}$, the initial global state of the backward process. If we set $\tilde{\rho}_{SE} = \Theta \rho_{SE}^* \Theta^\dagger$, then $\tilde{\varrho}_{m\mu} = \varrho_{m\mu}^*$ and $\Delta_\mathrm{i} s_\gamma$ becomes the inclusive entropy production per trajectory. Its average,

$$\begin{aligned}\langle \Delta_\mathrm{i} s_\gamma \rangle &= -\sum_{m,\mu} \varrho_{m\mu}^* \ln \varrho_{m\mu}^* + \sum_n p_n \ln p_n + \sum_\nu q_\nu \ln q_\nu \\ &= S(\rho_{SE}^*) - S(\rho_S) - S(\rho_E) = \Delta_\mathrm{i} S_\mathrm{inc},\end{aligned} \tag{27}$$

equals the inclusive entropy production defined in Eq. (10). If the initial condition for the backward process is the uncorrelated state $\tilde{\rho}_{SE} = \Theta(\rho_S^* \otimes \rho_E^*)\Theta^\dagger$, then $\tilde{\varrho}_{m\mu} = p_m^* q_\mu^*$ and $\Delta_\mathrm{i} s_\gamma$ is the noninclusive entropy production per trajectory, whose average yields the entropy production defined in Eq. (15),

$$\langle \Delta_\mathrm{i} s_\gamma \rangle = S(\rho_S^*) - S(\rho_S) + S(\rho_E^*) - S(\rho_E) = \Delta_\mathrm{i} S. \tag{28}$$

A third choice sets the environment in the (inverted) initial state of the forward process, $\tilde{\rho}_{SE} = \Theta(\rho_S^* \otimes \rho_E)\Theta^\dagger$, which yields $\tilde{\varrho}_{m\mu} = p_m^* q_\mu$. In this case, both initial and final local measurements in the environment are performed in the same basis $\mathcal{Q}_\mu^* = \mathcal{Q}_\mu$, and we obtain

$$\langle \Delta_\mathrm{i} s_\gamma \rangle = \Delta_\mathrm{i} S + S(\rho_E^* || \rho_E), \tag{29}$$

which includes an extra contribution measuring the disturbance on the environment during the process. The term $S(\rho_E^*||\rho_E)$, unlike $S(\rho_E^*) - S(\rho_E)$, is negligible when the environmental state is modified only infinitesimally (see Appendix A), as is the case, e.g., of a large reservoir. Moreover, when ρ_E is a Gibbs state, Eq. (29) is the entropy production proposed in Ref. [50], and $S(\rho_E^*||\rho_E)$ corresponds to the thermodynamic entropy production due to irreversibly resetting the ancilla back to ρ_E in contact with an equilibrium reservoir at the same temperature. Finally, we stress that for equilibrium canonical initial conditions both in the forward and in the backward processes, the trajectory entropy production (23) equals the stochastic dissipative work, and one recovers the celebrated Crooks work theorem and the original Jarzynski equality [6,7].

IV. DUAL PROCESSES: ADIABATIC AND NONADIABATIC ENTROPY PRODUCTION

We now focus on the reduced dynamics. Our aim is to obtain FT's involving only the quantum trajectory defined in Sec. III and the initial and final states of the system. To do that, we follow our previous work [33], where we derived a FT for CPTP maps based on the dual dynamics introduced by Crooks in Ref. [70]. Remarkably, the resulting FT goes beyond the one that we have obtained considering the global dynamics, Eq. (23), as it will reveal an interesting split of the total entropy production into two terms: the adiabatic entropy production, which accounts for the irreversibility of the stationary regime, and the nonadiabatic entropy production, which measures how far the system is from that stationary state.

We apply the formalism in Ref. [33] to $\mathcal{E}$, the map governing the reduced dynamics of the process, as well as to the map corresponding to the backward dynamics. Therefore, we first need to introduce the reduced dynamics in the backward process, which will be described by a new CPTP map $\tilde{\mathcal{E}}$. To do that, it is necessary that the system and the environment start the backward process in an uncorrelated state $\tilde{\rho}_{SE} = \tilde{\rho}_S \otimes \tilde{\rho}_E$; i.e., we have to impose $\tilde{I}_{m\mu} = 0$

[see Eq. (25)]. Otherwise, the CPTP map of the backward reduced dynamics would depend on the initial state of the system. In that case, similarly to our choice (8) for the forward process, a useful representation of $\tilde{\mathcal{E}}$ is

$$\tilde{\mathcal{E}}_{\nu\mu}(\tilde{\rho}_S) = \tilde{M}_{\nu\mu}\tilde{\rho}_S\tilde{M}^\dagger_{\nu\mu}, \tag{30}$$

where the backward Kraus operators are given by

$$\tilde{M}_{\nu\mu} = \sqrt{\tilde{q}_\mu}\langle\phi_\nu|_E\Theta_E^\dagger U_{\tilde{\Lambda}}\Theta_E|\phi^*_\mu\rangle_E. \tag{31}$$

Notice that here we have swapped subscripts with respect to the definition of the forward operators given by Eq. (8). This can be done since the pair (μ,ν) is just a label of the Kraus operator. The choice in Eq. (31) means that the operation $\tilde{\mathcal{E}}_{\nu\mu}$ is equivalent to obtaining μ in the initial measurement of the backward process and ν in the final one. Now, microreversibility (22) implies an intimate relationship between the forward and backward Kraus operators:

$$\Theta_S^\dagger\tilde{M}_{\nu\mu}\Theta_S = \sqrt{\tilde{q}_\mu}\langle\phi_\nu|_E U^\dagger_\Lambda|\phi^*_\mu\rangle_E = e^{-\sigma^E_{\mu\nu}/2}M^\dagger_{\mu\nu}. \tag{32}$$

It is important to notice that the FT for the total entropy production (23) can be derived directly from the above equation. In other words, Eq. (32) expresses the fundamental symmetry under time reversal, yielding the FT.

A. Dual-reverse process and nonadiabatic entropy production FT

In order to go beyond the FT for the total entropy production, we proceed as in Refs. [33,70]. These works, inspired by classical stochastic thermodynamics, introduce a quantum dual dynamics that reveals the irreversibility associated with a map at the steady state. In the following, we denote π as an invariant state of the forward map, $\mathcal{E}(\pi) = \pi$, which we indeed assume to be positive definite. The dual dynamics—which we call here dual-reverse dynamics, following the criterion used for classical systems [21–23]—is defined as a map $\tilde{\mathcal{D}}(\rho)$ such that $\tilde{\pi} \equiv \Theta_S\pi\Theta_S^\dagger$ is an invariant state, i.e., $\tilde{\mathcal{D}}(\tilde{\pi}) = \tilde{\pi}$. Furthermore, when the map is applied several times starting from the stationary state $\tilde{\pi}$, it generates trajectories $\tilde{\gamma}$ distributed as $\tilde{P}_D(\tilde{\gamma}|\tilde{\pi}) = P(\gamma|\pi)$. Here, the trajectories are $\gamma = \{n,(\nu_1,\mu_1),\ldots,(\nu_N,\mu_N),m\}$ and $\tilde{\gamma} = \{m,(\mu_N,\nu_N),\ldots,(\mu_1,\nu_1),n\}$, corresponding to N applications of the map.

Summarizing, in the stationary regime, the dual-reverse dynamics generates the same ensemble of trajectories as the forward process, but reversed in time. For instance, if the map describes the dynamics of a system in contact with a single thermal bath (thermalization), then the forward process generates reversible trajectories (indistinguishable from their reversal) and the dual-reverse map coincides with the forward map. In nonequilibrium situations, the dual generically inverts flows. For instance, for a system in contact with two thermal baths at different temperatures, the dual-reverse dynamics is usually obtained by swapping the temperatures of the baths, hence inverting the flow of heat.

In any case, one can prove that a Kraus representation of the dual-reverse map is given by the operators [33,70]

$$\tilde{D}_{\nu\mu} = \Theta_S\pi^{\frac{1}{2}}M^\dagger_{\mu\nu}\pi^{-\frac{1}{2}}\Theta_S^\dagger. \tag{33}$$

Finally, the dual-reverse process is the dual-reverse map complemented by a specific choice of the initial condition for the system (the environment does not appear explicitly in the dual map, which acts only on the system). The appropriate initial condition for the dual-reverse process is $\tilde{\rho}_S$, i.e., the same as the backward process.

We now have three processes: the forward $\mathcal{E}$, the backward $\tilde{\mathcal{E}}$, and the dual-reverse $\tilde{\mathcal{D}}$, each one inducing an evolution in the system characterized by trajectories $\gamma = \{n,\nu,\mu,m\}$. We can compute the probability of observing a trajectory γ or its reverse $\tilde{\gamma} = \{m,\mu,\nu,n\}$ in each of those evolutions. With a self-explanatory notation, these probabilities read

$$P(\gamma) = p_n\mathrm{Tr}[\mathcal{P}^*_m M_{\mu\nu}\mathcal{P}_n M^\dagger_{\mu\nu}], \tag{34}$$

$$\tilde{P}(\tilde{\gamma}) = \tilde{p}_m\mathrm{Tr}[\Theta_S\mathcal{P}_n\Theta_S^\dagger\tilde{M}_{\nu\mu}\Theta_S\mathcal{P}^*_m\Theta_S^\dagger\tilde{M}^\dagger_{\nu\mu}], \tag{35}$$

$$\tilde{P}_D(\tilde{\gamma}) = \tilde{p}_m\mathrm{Tr}[\Theta_S\mathcal{P}_n\Theta_S^\dagger\tilde{D}_{\nu\mu}\Theta_S\mathcal{P}^*_m\Theta_S^\dagger\tilde{D}^\dagger_{\nu\mu}]. \tag{36}$$

To obtain FT's from these expressions, we need a condition of proportionality between operators $M^\dagger_{\mu\nu}$ and $\tilde{D}_{\nu\mu}$, similar to the relationship (32) between $M^\dagger_{\mu\nu}$ and $\tilde{M}_{\nu\mu}$.

In Ref. [33] inspired by Ref. [71], we found that a necessary and sufficient condition for that proportionality is the following. We first define the nonequilibrium potential $\Phi = -\ln\pi$ from the invariant state π. Its spectral decomposition reads

$$\Phi = \sum_i \phi_i|\pi_i\rangle\langle\pi_i|, \tag{37}$$

where $\phi_i = -\ln\pi_i$, and π_i and $\{|\pi_i\rangle\}$ are, respectively, the eigenvalues and eigenstates of the invariant density matrix π. Now, we require that each Kraus operator $M_{\mu\nu}$ is unambiguously related to a nonequilibrium potential change $\Delta\phi_{\mu\nu}$ (note, however, that the converse statement is not necessarily true; i.e., we may, have for different values of μ and ν, the same value of $\Delta\phi_{\mu\nu}$). In the invariant-state eigenbasis, this condition reads

$$M_{\mu\nu} = \sum_{i,j} m^{\mu\nu}_{ij}|\pi_j\rangle\langle\pi_i|, \tag{38}$$

with $m_{ij}^{\mu\nu}=0$ whenever $\phi_j-\phi_i\neq\Delta\phi_{\mu\nu}$. As pointed out in Ref. [33], this condition does not imply single jumps between pairs of π eigenstates, but it could account for any set of correlated transitions between different pairs with the same associated $\Delta\phi_{\mu\nu}$. An extreme example is a unital map, where π is proportional to the identity matrix. In that case, $\Delta\phi_{\mu\nu}=0$, and any complex coefficients $m_{ij}^{\mu\nu}$ satisfy Eq. (38). It is not hard to show that condition (38) is equivalent to [33]

$$[\Phi,M_{\mu\nu}]=\Delta\phi_{\mu\nu}M_{\mu\nu},\qquad [\Phi,M_{\mu\nu}^{\dagger}]=-\Delta\phi_{\mu\nu}M_{\mu\nu}^{\dagger}. \tag{39}$$

This alternative formulation of Eq. (38) indicates that, when $\Delta\phi_{\mu\nu}\neq 0$, $M_{\mu\nu}$ can be interpreted as ladder operators in the eigenbasis of the invariant state π.

For thermalization or Gibbs preserving maps, with $\pi=e^{-\beta(H-F)}$, $\beta=(kT)^{-1}$ being the inverse temperature and F the equilibrium free energy, the potential is $\Phi=\beta(H-F)$ and $kT\Delta\Phi$ is the energy transfer between the system and the environment, i.e., the heat. In this case, condition (38) implies that the Kraus operators produce jumps between levels with the same energy spacing or, equivalently, jumps with a well-defined value of the heat.

Introducing condition (38) in Eq. (33), one easily derives the following relationship between the forward and the dual-reverse Kraus operators [33]:

$$\Theta_S^{\dagger}\tilde{D}_{\nu\mu}\Theta_S=e^{\Delta\phi_{\mu\nu}/2}M_{\mu\nu}^{\dagger}, \tag{40}$$

and, using Eq. (32), one gets

$$\tilde{D}_{\nu\mu}=e^{(\sigma_{\mu\nu}^{E}+\Delta\phi_{\mu\nu})/2}\tilde{M}_{\nu\mu}. \tag{41}$$

Finally, inserting Eqs. (40) and (41) into the expressions for the probability of trajectories, Eqs. (34)–(36), we obtain the following FT's:

$$\Delta_{\mathrm{i}}s_{\gamma}^{\mathrm{na}}\equiv\ln\frac{P(\gamma)}{\tilde{P}_D(\tilde{\gamma})}=\sigma_{nm}^{S}-\Delta\phi_{\mu\nu}, \tag{42}$$

$$\Delta_{\mathrm{i}}s_{\mu\nu}^{\mathrm{a}}\equiv\ln\frac{\tilde{P}_D(\tilde{\gamma})}{\tilde{P}(\tilde{\gamma})}=\sigma_{\mu\nu}^{E}+\Delta\phi_{\mu\nu}. \tag{43}$$

We call $\Delta_{\mathrm{i}}s_{\mu\nu}^{\mathrm{a}}$ the adiabatic entropy production and $\Delta_{\mathrm{i}}s_{\mu\nu}^{\mathrm{na}}$ the nonadiabatic entropy production, following the terminology used in classical stochastic thermodynamics [21–23]. They contribute to the total entropy production per trajectory, $\Delta_{\mathrm{i}}s_{\gamma}=\Delta_{\mathrm{i}}s_{\mu\nu}^{\mathrm{a}}+\Delta_{\mathrm{i}}s_{\gamma}^{\mathrm{na}}$, as defined in Eq. (23). Below, we discuss the averages of the adiabatic and nonadiabatic entropy production in some cases, clarifying the origin of the terms.

B. Dual process and adiabatic entropy production FT

Notice that Eq. (43) is not a proper FT for the forward process. In particular, we cannot derive a Jarzynski-like equality for $\exp(\Delta_{\mathrm{i}}s_{\mu\nu}^{\mathrm{a}})$ averaged over forward trajectories, $P(\gamma)$. To achieve this goal, we need a further assumption that will allow us to apply the results of Ref. [33] to the backward process. In this way, we obtain the dual reverse of the backward process, which we simply call the dual map $\mathcal{D}$. If condition (38) is satisfied, then, by virtue of Eq. (32), the backward Kraus operators can be written as

$$\begin{aligned}\tilde{M}_{\nu\mu}&=e^{-\sigma_{\mu\nu}^{E}/2}\sum_{i,j}(m_{ij}^{\mu\nu})^{*}\Theta_S|\pi_i\rangle\langle\pi_j|\Theta_S^{\dagger}\\&=\sum_{i,j}\tilde{m}_{ij}^{\nu\mu}|\tilde{\pi}_j\rangle\langle\tilde{\pi}_i|,\end{aligned} \tag{44}$$

with $\tilde{m}_{ij}^{\nu\mu}\equiv e^{-\sigma_{\mu\nu}^{E}/2}(m_{ji}^{\mu\nu})^{*}$. We observe that, setting $\Delta\tilde{\phi}_{\nu\mu}=-\Delta\phi_{\mu\nu}$, condition (38) is recovered for the backward process. However, a requirement to apply the theoretical framework developed in Ref. [33] is that $|\tilde{\pi}\rangle\equiv\Theta_S|\pi\rangle$ is an invariant state of the backward map $\tilde{\mathcal{E}}$. This is not warranted by the definition of $\tilde{\mathcal{E}}$, not even when the Kraus operators are of the form (38). Therefore, we have to add this extra assumption. In particular, it is satisfied when the driving protocol associated with the map is time symmetric, the Hamiltonian of the environment is invariant under time reversal, and we perform the same measurements at the beginning and the end of the process on the environment. This is the case of the infinitesimal maps that govern the dynamics of a quantum Markov process since, even in the case of arbitrary driving, each map is generated by a constant Hamiltonian.

We now obtain the dual operators $D_{\mu\nu}$, applying transformation (33) to the backward Kraus operators $\tilde{M}_{\nu\mu}$ (with the role of Θ_S and $\Theta_S^{\dagger}$ swapped [33]). Similarly to Eq. (40), condition (38) on the backward operators implies

$$\Theta_S D_{\mu\nu}\Theta_S^{*}=e^{\Delta\tilde{\phi}_{\nu\mu}/2}\tilde{M}_{\nu\mu}^{\dagger}=e^{-\Delta\phi_{\mu\nu}/2}\tilde{M}_{\nu\mu}^{\dagger}, \tag{45}$$

and, using Eq. (32),

$$D_{\mu\nu}=e^{-(\sigma_{\mu\nu}^{E}+\Delta\phi_{\mu\nu})/2}M_{\mu\nu}. \tag{46}$$

The dual process is given by the dual map with initial condition ρ_S. The trajectories generated by this process are distributed as

$$P_D(\gamma)=p_n\mathrm{Tr}_S[\mathcal{P}_m^{*}D_{\mu\nu}\mathcal{P}_nD_{\mu\nu}^{\dagger}]. \tag{47}$$

Combining Eqs. (34) and (47) and using condition (32), we get a new FT for the adiabatic entropy production:

$$\Delta_{\mathrm{i}}s_{\mu\nu}^{\mathrm{a}}=\ln\frac{P(\gamma)}{P_D(\gamma)}=\sigma_{\mu\nu}^{E}+\Delta\phi_{\mu\nu}. \tag{48}$$

C. Integral fluctuation theorems

We can now derive integral FT's for the adiabatic and nonadiabatic entropy productions:

$$\langle e^{-\Delta_i s^{na}}\rangle = 1, \qquad \langle e^{-\Delta_i s^{a}}\rangle = 1, \tag{49}$$

which follow from the detailed versions by averaging over trajectories γ. Finally, convexity of the exponential function provides the following two second-law-like inequalities as a corollary $\langle \Delta_i s_\gamma^{na}\rangle \geq 0$ and $\langle \Delta_i s_\gamma^{a}\rangle \geq 0$. As for the FT for the total entropy production (23), the meaning of these average entropies becomes clearer if the initial condition of the backward process is specified. Setting $\tilde{\rho} = \Theta(\rho_S^* \otimes \rho_E^*)\Theta^\dagger$, the average of the adiabatic and nonadiabatic entropy production defined by Eqs. (40) and (41) reads

$$\Delta_i S_{na} \equiv \langle \Delta_i s_\gamma^{na}\rangle = S(\rho_S^*) - S(\rho_S) - \langle \Delta\phi\rangle \geq 0, \tag{50}$$

$$\Delta_i S_{a} \equiv \langle \Delta_i s_\gamma^{a}\rangle = S(\rho_E^*) - S(\rho_E) + \langle \Delta\phi\rangle \geq 0, \tag{51}$$

and the sum equals the total noninclusive average entropy production $\Delta_i S$ [see Eq. (15)]. It is interesting to notice that the average change of the potential,

$$\langle \Delta\phi\rangle = \sum_{\mu,\nu} P(\gamma)\Delta\phi_{\mu\nu} = \sum_{\mu,\nu} \mathrm{Tr}[M_{\mu\nu}\rho_S M_{\mu\nu}^\dagger]\Delta\phi_{\mu\nu}, \tag{52}$$

can be alternatively written in terms of averages over the states of the system, ρ_S' and ρ_S, if condition (38) is fulfilled. That condition implies $[\Phi, M_{\mu\nu}] = M_{\mu\nu}\Delta\phi_{\mu\nu}$ (see also Ref. [33]). We introduce the commutator in Eq. (52),

$$\begin{aligned}\langle \Delta\phi\rangle &= \sum_{\mu,\nu} \mathrm{Tr}[(\Phi M_{\mu\nu} - M_{\mu\nu}\Phi)\rho_S M_{\mu\nu}^\dagger] \\ &= \mathrm{Tr}[\Phi(\rho_S' - \rho_S)],\end{aligned} \tag{53}$$

where we have used the cyclic property of the trace and Eqs. (7) and (8). Therefore, the average potential change $\langle \Delta\phi\rangle$ can be expressed as the change in the expected value of the operator Φ due to the map. Recall that the operator Φ acts on the Hilbert space of the system $\mathcal{H}_S$, i.e., is a local observable on the system.

If the final measurement does not alter the state of the system, i.e., if $\rho_S^* = \rho_S'$, or if the final measurement is skipped, as is the case when we concatenate maps and the system is measured only after the whole concatenation (see Sec. IV E), we can write the average nonadiabatic entropy production in an appealing form:

$$\begin{aligned}\Delta_i S_{na} &= S(\rho_S') - S(\rho_S) - \langle \Delta\phi\rangle \\ &= \mathrm{Tr}[\rho_S(\ln\rho_S + \Phi)] - \mathrm{Tr}[\rho_S'(\ln\rho_S' + \Phi)] \\ &= S(\rho_S||\pi) - S(\rho_S'||\pi) \geq 0,\end{aligned} \tag{54}$$

where we have used the definition $\Phi = -\ln\pi$ of the potential operator in terms of the invariant state π. Here, we see that the nonadiabatic entropy production is related to the distance between the state of the system and the invariant state π. During the evolution, the state of the system can only approximate the invariant state, and the nonadiabatic entropy production is a measure of the irreversibility associated with such convergence. In fact, inequality in Eq. (54) follows from direct application of Ulhman's inequality (monotonicity of quantum relative entropy) holding for general CPTP evolutions [51,62].

D. Multipartite environments

The results obtained so far can also be applied to a multipartite environment. The corresponding Hilbert space is decomposed as $\mathcal{H}_E = \bigotimes_{r=1}^R \mathcal{H}_r$, corresponding to R independent ancillas or reservoirs interacting with the open system. We assume an uncorrelated initial state of the environment, $\rho_E = \rho_1 \otimes \ldots \otimes \rho_R$, and that the measurements are performed locally in each environmental ancilla.

In this case, the adiabatic entropy production per trajectory and its average read (see details in Appendix B)

$$\Delta_i s_{\mu\nu}^{a} = \sum_{r=1}^{R} \sigma^r_{\mu^{(r)}\nu^{(r)}} + \Delta\phi_{\mu\nu}, \tag{55}$$

$$\Delta_i S_{a} = \sum_{r=1}^{R} S(\rho_r^*) - S(\rho_r) + \langle \Delta\phi\rangle \geq 0. \tag{56}$$

E. Concatenation of CPTP maps

Up to now, we have considered a single interaction of duration τ between the system and the environment [see Eq. (2)]. The CPTP map $\mathcal{E}$ describes the evolution of the system when the environment is measured before and after the interaction. This framework can be extended to concatenations of CPTP maps, where the system interacts sequentially with the environment. Each single interaction in a time interval $[t, t+\tau]$ is described by a single CPTP map like $\mathcal{E}$. The map describing the reduced dynamical evolution for N interactions, from $t = 0$ to $t = N\tau$, is

$$\Omega = \mathcal{E}^{(N)} \circ \cdots \circ \mathcal{E}^{(l)} \circ \cdots \circ \mathcal{E}^{(1)}, \tag{57}$$

where, in particular, each map $\mathcal{E}^{(l)}$ may have a different (positive-definite) invariant state $\pi^{(l)}$. We assume that the system interacts from time $t_{l-1} \equiv (l-1)\tau$ to time $t_l \equiv l\tau$ with a "fresh" (uncorrelated) environment in a generic state $\rho_E^{(l)} \equiv \sum_\alpha q_\alpha^{(l)} \mathcal{Q}_\alpha^{(l)}$, and, as in the single map case, the environment is measured before and after interaction with the system by projective measurements. On the other hand, the system is only measured at the

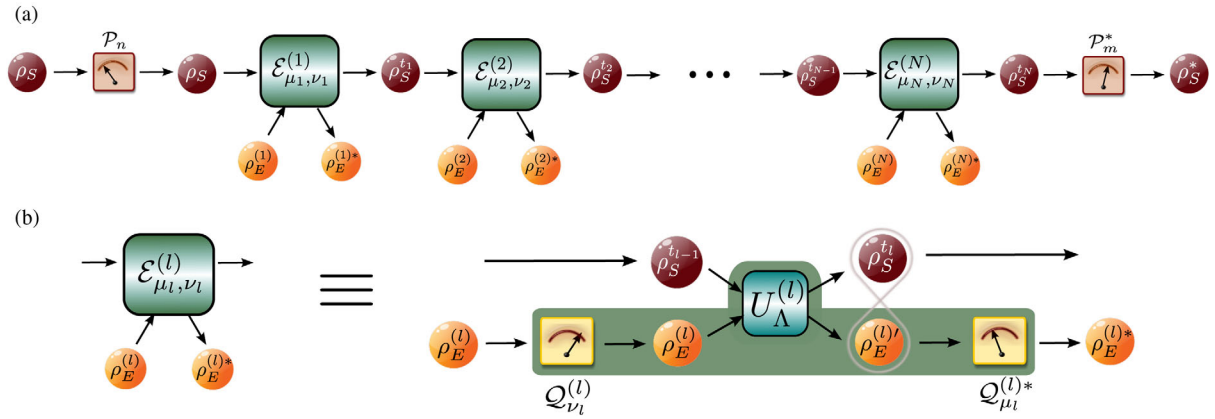

FIG. 2. (a) Schematic diagram of a trajectory generated by the map concatenation. Projective measurements on the system are only performed at the beginning and at the end of the concatenation. (b) Any operation $\mathcal{E}^{(l)}_{\mu_l,\nu_l}$ in the concatenation consists in the interaction of the system with an environmental ancilla in the state $\rho_E^{(l)}$ via the unitary $\hat{U}^{(l)}_\Lambda$ depending on the protocol Λ_l. The ancilla is measured before and after interaction, generating outcomes ν_l and μ_l, respectively.

beginning and end of the whole concatenation (57), as depicted in Fig. 2.

In this case, trajectories are specified by the set of outcomes $\gamma = \{n, (\nu_1, \mu_1), \ldots, (\nu_N, \mu_N), m\}$, which can be compared to the backward trajectories $\tilde{\gamma} = \{m, (\nu_N, \mu_N), \ldots, (\nu_1, \mu_1), n\}$ generated by the reverse sequence of maps $\tilde{\Omega} = \tilde{\mathcal{E}}^{(1)} \circ \cdots \circ \tilde{\mathcal{E}}^{(l)} \circ \cdots \circ \tilde{\mathcal{E}}^{(N)}$. We find that all of our above results apply as well to the concatenations setup (see Appendix C), yielding the following three detailed fluctuation theorems:

$$\Delta_{\mathrm{i}} s^{\mathrm{na}}_\gamma = \ln \frac{P(\gamma)}{\tilde{P}_D(\tilde{\gamma})} = \sigma^S_{nm} - \sum_{l=1}^{N} \Delta\phi^{(l)}_{\mu_l\nu_l}, \tag{58}$$

$$\Delta_{\mathrm{i}} s^{\mathrm{a}}_\gamma = \ln \frac{P(\gamma)}{P_D(\gamma)} = \sum_{l=1}^{N} (\sigma^E_{\mu_l\nu_l} + \Delta\phi^{(l)}_{\mu_l\nu_l}), \tag{59}$$

$$\Delta_{\mathrm{i}} s_\gamma = \ln \frac{P(\gamma)}{\tilde{P}(\tilde{\gamma})} = \Delta_{\mathrm{i}} s^{\mathrm{na}}_\gamma + \Delta_{\mathrm{i}} s^{\mathrm{a}}_\gamma, \tag{60}$$

where σ^S_{nm} is given by Eq. (24), $\sigma^E_{\mu_l\nu_l} = \ln q^{(l)}_{\nu_l} - \ln \tilde{q}^{(l)}_{\mu_l}$ is the entropy change in the environment due to the lth map, and $\Delta\phi^{(l)}_{\mu\nu} = -\ln \pi^{(l)}_\mu + \ln \pi^{(l)}_\nu$ is the change in nonequilibrium potential for the lth map.

V. LINDBLAD MASTER EQUATIONS

The results of the last section can be applied to Lindblad master equations [31,52]. Consider the following master equation in Lindblad form [4,60,72], depending on an external parameter λ_t:

$$\dot{\rho}_t = -\frac{i}{\hbar}[H, \rho] + \sum_{k=1}^{K} \left(L_k \rho_t L_k^\dagger - \frac{1}{2}\{L_k^\dagger L_k, \rho_t\} \right) \equiv \mathcal{L}_{\lambda_t} \rho_t, \tag{61}$$

where $H(\lambda_t)$ is the system Hamiltonian in the selected picture and $L_k(\lambda_t)$ are positive Lindblad operators, which generally depend on the control parameter λ_t and describe jumps in some (possibly time-dependent) basis. We assume that there exists an instantaneous invariant state π_λ, which is the steady state of Eq. (61) when the external control parameter is frozen: $\mathcal{L}_\lambda \pi_\lambda = 0$ [5].

The Lindblad equation (61) can be written as a concatenation of CPTP maps,

$$\rho_{t+dt} = (\mathbb{I}_S + dt\mathcal{L}_{\lambda_t})\rho_t \equiv \mathcal{E}(\rho_t), \tag{62}$$

with the Kraus representation

$$M_0(\lambda_t) \equiv \mathbb{I}_S - dt\left(\frac{i}{\hbar} H + \frac{1}{2} \sum_{k=1}^{K} L_k^\dagger(\lambda_t) L_k(\lambda_t) \right), \tag{63}$$

$$M_k(\lambda_t) \equiv \sqrt{dt} L_k(\lambda_t), \qquad k = 1, \ldots, K. \tag{64}$$

Recall that this Kraus representation is not unique [60]. As before, the representation in Eqs. (63) and (64) is related to a specific detection scheme for the jumps; that is, it implies a specific choice of the initial state and the local observables to be monitored in the environment (the set of projectors $\{\mathcal{Q}_\nu\}$ and $\{\mathcal{Q}^*_\mu\}$).

The Kraus representation in Eqs. (63) and (64) is based on a family of operations M_k, with $k = 1, \ldots, K$, that induce jumps in the state of the system and occur with probabilities of order dt, and a single operation M_0 that induces a smooth nonunitary evolution and occurs with probability of order 1. This implies that a trajectory γ consists of a large number of 0's punctuated by a few jumps M_k, with $k = 1, \ldots, K$. An alternative way of describing the trajectory is to specify the jumps k_j and the times t_j where

they occur, i.e., $\gamma=\{n,(k_1,t_1),\ldots,(k_j,t_j),\ldots,(k_N,t_N),m\}$, where, as before, n and m denote the outcomes of the initial and final measurements in the system at times $t=0$ and $t=t_f$. Jump k is given by the operation $\mathcal{E}_k(\rho)\equiv M_k\rho M_k^\dagger$, whereas between two consecutive jumps at t_j and t_{j+1}, the evolution is given by the repeated application of the operation corresponding to the Kraus operator $M_0(\lambda_t)$ in Eq. (63). This results in a smooth evolution given by the operator

$$U_{\rm eff}(t_{j+1},t_j)=\mathcal{T}_+\exp\left(-\frac{i}{\hbar}\int_{t_j}^{t_{j+1}}ds\,H_{\rm eff}(\lambda_s)\right), \quad (65)$$

with an effective non-Hermitian Hamiltonian that reads

$$H_{\rm eff}(\lambda_t)=H(\lambda_t)-\frac{i\hbar}{2}\sum_{k=1}^{K}L_k^\dagger(\lambda_t)L_k(\lambda_t). \quad (66)$$

In this representation, the probability of a trajectory $\gamma=\{n,(k_1,t_1),\ldots,(k_j,t_j),\ldots,(k_N,t_N),m\}$ is

$$P(\gamma)=\mathrm{Tr}[\mathcal{P}_m^*\mathcal{U}_{t_f,t_N}\mathcal{E}_{k_N}\mathcal{U}_{t_N,t_{N-1}}\ldots \times\mathcal{E}_{k_l}\ldots\mathcal{U}_{t_2,t_1}\mathcal{E}_{k_1}\mathcal{U}_{t_1,0}(\mathcal{P}_n\rho_0\mathcal{P}_n)], \quad (67)$$

with $\mathcal{U}_{t_{j+1},t_j}(\rho)=U_{\rm eff}(t_{j+1},t_j)\rho U_{\rm eff}^\dagger(t_{j+1},t_j)$.

A. Backward, dual, and dual-reverse dynamics

Consider now the backward dynamics. The time inversion of the evolution of the global system corresponds to a time-reversed version of the Lindblad master equation (61). As in the previous section, the backward process is generated by inverting the sequence of operations together with the time inversion of each operation in the sequence. The map corresponding to an infinitesimal time step in the time-reversed dynamics, $\tilde\rho_{t+dt}=\tilde{\mathcal{E}}(\tilde\rho_t)$, admits a Kraus representation with Kraus operators $\tilde M_k(\lambda_t)$. To obtain the backward map, we would need to know details about the environment that induces the Markovian dynamics given by the Lindblad equation (61). However, in the previous sections, we have derived a relationship between the forward and backward CPTP maps, namely, Eq. (32):

$$\tilde M_0=e^{-\sigma_0^E/2}\Theta_S M_0^\dagger\Theta_S^\dagger, \quad (68)$$

$$\tilde M_k=e^{-\sigma_k^E/2}\Theta_S M_k^\dagger\Theta_S^\dagger. \quad (69)$$

Imposing the backward maps to be trace preserving, that is, $\tilde M_0^\dagger\tilde M_0+\sum_k\tilde M_k^\dagger\tilde M_k=\mathbb{I}$, we obtain $\sigma_0^E=0$, and the consistency condition

$$\sum_{k=1}^{K}(L_k^\dagger L_k-L_k{L_k}^\dagger e^{-\sigma_k^E})=0. \quad (70)$$

Any set of numbers $\{\sigma_k^E\}$ satisfying Eq. (70) defines, through Eq. (68), an admissible backward process. The existence of such a set is warranted since any Lindblad equation can be derived from the interaction between the system and an ancilla.

For any trajectory $\gamma=\{n,(k_1,t_1),\ldots,(k_N,t_N),m\}$ generated in the forward process with probability $P(\gamma)$, there exists a backward trajectory $\tilde\gamma=\{m,(k_N,t_N),\ldots,(k_1,t_1),n\}$ occurring in the backward process with probability $\tilde P(\tilde\gamma)$. The backward trajectory can also be identified by the times of successive jumps. In this representation, the probability of trajectory $\tilde\gamma$ can be written as

$$\tilde P(\tilde\gamma)=\mathrm{Tr}[\Theta_S\mathcal{P}_n\Theta_S^\dagger\tilde{\mathcal{U}}_{t_1,0}\tilde{\mathcal{E}}_{k_1}\tilde{\mathcal{U}}_{t_2,t_1}\ldots\tilde{\mathcal{E}}_{k_l}\ldots \times\tilde{\mathcal{U}}_{t_N,t_{N-1}}\tilde{\mathcal{E}}_{k_N}\tilde{\mathcal{U}}_{t_f,t_N}(\Theta_S\mathcal{P}_m^*\rho_{t_f}\mathcal{P}_m^*\Theta_S^\dagger)], \quad (71)$$

where $\tilde{\mathcal{E}}_k(\tilde\rho)=\tilde M_k\tilde\rho\tilde M_k^\dagger$. The smooth evolution between jumps $\tilde{\mathcal{U}}_{t',t}(\tilde\rho_t)=\tilde U_{\rm eff}(t',t)\tilde\rho_t\tilde U_{\rm eff}^\dagger(t',t)$ is given by the operator

$$\tilde U_{\rm eff}(t',t)=\mathcal{T}_+\exp\left(\frac{i}{\hbar}\int_t^{t'}ds\,\Theta_S H_{\rm eff}^\dagger(\tilde\lambda_s)\Theta_S^\dagger\right), \quad (72)$$

where $\{\tilde\lambda_t\}$ again corresponds to the inverse sequence of values for the control parameter. It can be shown that this smooth evolution obeys the microreversibility relationship $\Theta_S^\dagger\tilde U_{\rm eff}(t',t)\Theta_S=U_{\rm eff}(t',t)^\dagger$.

Let us discuss now the dual and dual-reverse dynamics. The condition (39), which is necessary to define the dual-reverse process, reads [31,52]

$$[\Phi,L_k]=\Delta\phi_k L_k,\qquad [\Phi,L_k^\dagger]=-\Delta\phi_k L_k^\dagger. \quad (73)$$

These commutation relationships indicate that the Lindblad operators $L_k(\lambda_t)$ promote jumps between the eigenstates of π_{λ_t}. Furthermore, as the condition must be fulfilled for the operator M_0 in Eq. (63) as well, we need $[H,\sum_k L_k^\dagger L_k]=[H,\Phi]=0$, which in turn implies $\Delta\phi_0=0$. This means that the instantaneous steady state of the dynamics must be diagonal in the basis of the Hamiltonian term appearing in Eq. (61). This condition is fulfilled by equilibrium Lindblad equations and in situations in which the operator H becomes the identity operator in an appropriate interaction picture (see, e.g., Refs. [45,73]). However, the condition can be broken in nonequilibrium situations, a genuine quantum effect. In Sec. VI C, we present an example of a periodically driven cavity mode where the adiabatic entropy production can be negative. Finally, as discussed in Sec. IV B, we recall that the fluctuation theorem for the adiabatic entropy production can be stated when the backward maps $\tilde{\mathcal{E}}$ admits $\tilde\pi_\lambda\equiv\Theta_S\pi_\lambda\Theta_S^\dagger$ as an invariant state.

If these conditions are fulfilled, the dual process is defined by the dual operations $\mathcal{D}_k(\cdot) = D_k(\cdot)D_k^\dagger$ with Kraus operators $\{D_k\}$ as defined in Eq. (46), whereas the dual-reverse process is given by operations $\tilde{\mathcal{D}}_k = \tilde{D}_k(\cdot)\tilde{D}_k^\dagger$ with Kraus operators $\{\tilde{D}_k\}$ defined in Eq. (40) [see also Eqs. (C7) and (C8) in Appendix C]. The probability of a trajectory γ in the dual process, $P_D(\gamma)$, can be calculated from Eq. (67) by using the same map $\mathcal{U}_{t',t}$ for the no-jump time evolution intervals and by replacing the operations $\mathcal{E}_k$ by the dual operations $\mathcal{D}_k$. Analogously, for the dual-reverse process, the probability of trajectory $\tilde{\gamma}$, $\tilde{P}_D(\tilde{\gamma})$, can be constructed from Eq. (71) with $\tilde{\mathcal{U}}_{t',t}$ for the no-jump evolution and dual-reverse operations $\tilde{\mathcal{D}}_k$. We further notice that, in general, $D_k \neq M_k$ and $\tilde{D}_k \neq \tilde{M}_k$; that is, $\sigma_k^E \neq -\Delta\phi_k$.

In many applications, the Lindblad operators come in pairs, and the corresponding pair of terms in the sum (70) cancel. This occurs if, for a specific pair of operators $\{L_i, L_j\}$, we have $L_i = \sqrt{\Gamma_i}L$ and $L_j = \sqrt{\Gamma_j}L^\dagger$, with $\Gamma_i(\lambda_t)$ and $\Gamma_j(\lambda_t)$ being positive transition rates, and $L(\lambda_t)$ some arbitrary (possibly time-dependent) system operator. Then, condition (70) implies (cf. Ref. [74])

$$\begin{aligned}\sigma_i^E(\lambda_t) &= \ln(\Gamma_i/\Gamma_j),\\ \sigma_j^E(\lambda_t) &= \ln(\Gamma_j/\Gamma_i) = -\sigma_i^E(\lambda_t),\end{aligned} \tag{74}$$

and the (inverted) Kraus operators of the backward map are also operators of the forward map:

$$\Theta_S^\dagger \tilde{M}_i \Theta_S = e^{-\sigma_i^E/2}M_i^\dagger = \sqrt{dt}e^{-\sigma_i^E/2}L_i^\dagger = \sqrt{dt}L_j = M_j, \tag{75}$$

where we have used the detailed-balance relation (32). Moreover, $\tilde{\pi}_\lambda \equiv \Theta\pi_\lambda\Theta^\dagger$ is invariant under the backward map:

$$\tilde{\mathcal{E}}(\tilde{\pi}_\lambda) = \sum_k \tilde{M}_k\Theta_S\pi_\lambda\Theta_S^\dagger\tilde{M}_k^\dagger = \sum_k \Theta_S M_k\pi_\lambda M_k^\dagger\Theta_S^\dagger = \tilde{\pi}_\lambda. \tag{76}$$

B. Entropy production rates

The above considerations lead us to reproduce the three different detailed FT's in Eq. (60) for quantum trajectories generated by Lindblad master equations. From the integral fluctuation theorems, we can derive second-law-like inequalities analogous to Eqs. (50) and (51) for the entropy production rates [31]:

$$\dot{S}_\mathrm{i} = \dot{S}_\mathrm{na} + \dot{S}_\mathrm{a} = \dot{S} + \langle\dot{\sigma}^E\rangle \geq 0, \tag{77}$$

$$\dot{S}_\mathrm{na} = \dot{S} - \dot{\phi} \geq 0, \qquad \dot{S}_\mathrm{a} = \langle\dot{\sigma}^E\rangle + \dot{\phi} \geq 0, \tag{78}$$

where $\dot{S} = -\mathrm{Tr}[\dot{\rho}_t \ln\rho_t]$ is the derivative of the von Neumann entropy of the system, $\dot{\phi} \equiv \mathrm{Tr}[\dot{\rho}_t\Phi(\lambda_t)] = -\mathrm{Tr}[\dot{\rho}_t \ln\pi_{\lambda_t}]$ is the nonequilibrium potential change rate, and $\langle\dot{\sigma}^E(\lambda_t)\rangle dt = \sum_{k_l}\mathrm{Tr}[\mathcal{E}_{k_l}(\rho_t)]\sigma_{k_l}^E(\lambda_t)$ the entropy change in the monitored environment during dt [52]. The three above equations guarantee the monotonicity of the average entropy production, $\Delta_\mathrm{i}S$, and the adiabatic and nonadiabatic contributions, $\Delta_\mathrm{i}S_\mathrm{na}$ and $\Delta_\mathrm{i}S_\mathrm{a}$, during the whole evolution.

The physical interpretation of the adiabatic and nonadiabatic entropy production now becomes clear. The nonadiabatic part can be written as

$$\dot{S}_\mathrm{na} = \mathrm{Tr}[\dot{\rho}_t(\ln\pi_{\lambda_t} - \ln\rho_t)], \tag{79}$$

which is the continuous time version of Eq. (54). If the control parameter changes quasistatically, we have $\rho_t \simeq \pi_{\lambda_t}$; therefore, the nonadiabatic entropy production vanishes. This is analogous to the classical nonadiabatic entropy production introduced in Refs. [20–23]. On the other hand, the adiabatic contribution $\dot{S}_\mathrm{a}$ is, in general, different from zero even if the driving is extremely slow. In a physical system, this term accounts for the entropy production required to keep the system out of equilibrium when λ is fixed, and the associated dissipated energy is usually referred to as housekeeping heat [20].

At this point, it is worth remarking an important difference between classical and quantum systems. In classical systems, the split of the entropy production in two terms, adiabatic and nonadiabatic, can always be done at the level of trajectories, and both terms obey fluctuation theorems that ensure the positivity of their respective averages. This is possible for quantum systems only if Eq. (39) [or Eq. (73) for Lindblad operators] is met. One can still use Eq. (79) as a definition for the average nonadiabatic entropy production $\dot{S}_\mathrm{na}$ and $\dot{S}_\mathrm{a} = \dot{S}_\mathrm{i} - \dot{S}_\mathrm{na}$ for the average adiabatic entropy production rate. However, these definitions cannot be extended to single trajectories; furthermore, they do not obey a fluctuation theorem. In the next section, we discuss a specific example where the condition is not fulfilled and, as a consequence, the average adiabatic entropy production rate can be negative.

Finally, it is also important to notice that $\dot{S}$ and $\langle\dot{\sigma}^E\rangle$ in Eq. (77) are exact differentials, i.e., can be written as the time derivative of the system and the environment entropy, respectively. On the other hand, the term $\dot{\phi} \equiv \mathrm{Tr}[\dot{\rho}_t\Phi(\lambda_t)]$, as well as the adiabatic and nonadiabatic entropy production rates in Eq. (78), cannot be expressed, in general, as a time derivative. One important exception is the case of a constant invariant state $\pi_{\lambda_t} = \pi$ like, for instance, in a relaxation in the absence of driving. In that case, all the quantities in Eqs. (77) and (78) are exact differentials. In particular, the nonadiabatic entropy production when the system relaxes from ρ_0 to ρ_t is given by

$$\Delta S_\mathrm{na} = -S(\rho_\tau||\pi) + S(\rho_0||\pi) \geq 0, \tag{80}$$

which equals $\Delta S_{\rm na} = S(\rho_0||\pi)$ for a full relaxation to $\rho_\tau = \pi$. The latter coincides with the entropy production introduced by Spohn [75].

VI. EXAMPLES

We illustrate our findings with three paradigmatic examples. In the first one, we consider a two-qubit CNOT gate as a simple process with a finite-size environment to illustrate the differences between the inclusive and noninclusive entropy production introduced in Sec. II C. The second and third examples correspond to two representative examples of nonequilibrium quantum Markov systems. The second example is an autonomous system coupled to several thermal baths. In this case, the nonadiabatic entropy production is zero except during the transient relaxation to the steady state. However, it provides an intuitive picture of how entropy is produced in nonequilibrium setups. The third example is a driven system that does not fulfill condition (38) and, consequently, does not admit the splitting of the entropy into adiabatic and nonadiabatic contributions with positive averages.

A. Two-qubit CNOT gate

The difference between the inclusive and noninclusive entropy production introduced in Sec. II C becomes especially relevant for processes where the system of interest repeatedly interacts with a finite-size reservoir. As an extreme case, we consider both the system and environment to be qubits with the same energy spacing ϵ. Their Hamiltonians are given by $H_S = \epsilon|1\rangle\langle 1|_S$ and $H_E = \epsilon|1\rangle\langle 1|_E$. We assume that the initial state of the system is partially coherent, $\rho_S = (\mathbb{I} + \alpha\sigma_x)/2$, with $0 \le \alpha \le 1$, and the environmental qubit starting in a thermal state $\rho_E = e^{-\beta H_E}/Z_E$ at inverse temperature $\beta = 1/k_B T \ge 0$, with $Z_E = 1 + e^{-\beta\epsilon}$ being the partition function. The initial state can be written as

$$\rho_{SE} = \rho_S \otimes \rho_E = \frac{1}{4}(\mathbb{I} + \alpha\sigma_x) \otimes (\mathbb{I} + \kappa\sigma_z), \quad (81)$$

where $\kappa \equiv \tanh(\beta\epsilon/2)$, σ_j with $j = x, y, z$ are the Pauli matrices, and we take the standard qubit basis $\{|0\rangle, |1\rangle\}$ for both the system and the environment. The eigenbasis of ρ_{SE} determines the projectors of the initial measurements $\{\mathcal{P}_n, \mathcal{Q}_\nu\}$, which are, in this case, $\mathcal{P}_\pm = |\psi_\pm\rangle\langle\psi_\pm|$ with $|\psi_\pm\rangle = (|0\rangle \pm |1\rangle)/\sqrt{2}$ and $\mathcal{Q}_\nu = |\nu\rangle\langle\nu|$ with $\nu = 0, 1$.

The system and environment interact through a CNOT gate, $U_{\rm CNOT}$, where the system acts as the control qubit [62]. The interaction leads to the following global system-environment state:

$$\rho'_{SE} = U_{\rm CNOT}(\rho_S \otimes \rho_E)U^\dagger_{\rm CNOT} = \frac{1}{4}(\mathbb{I} + \alpha\sigma_x \otimes \sigma_x - \alpha\kappa\sigma_y \otimes \sigma_y + \kappa\sigma_z \otimes \sigma_z). \quad (82)$$

Notice that ρ'_{SE} has maximally mixed reduced states both in the system and the environment. As a consequence, for any choice of the final projectors $\{\mathcal{P}^*_m, \mathcal{Q}^*_\mu\}$, we have $\rho'_S = \rho^*_S = \rho'_E = \rho^*_E = \mathbb{I}/2$. In contrast, the global state ρ^*_{SE} depends on the final projectors. The average work done during the interaction is $W = \mathrm{Tr}[(H_S + H_E)(\rho'_{SE} - \rho_{SE})] = \epsilon(1/2 - e^{-\beta\epsilon}/Z_E) > 0$, while there is no further energy contribution from local measurements.

The inclusive entropy production in Eq. (14) is just given by the erasure of quantum correlations in the final measurements, $\Delta_{\rm i} S_{\rm inc} = \mathcal{I}(\rho'_{SE}) - \mathcal{I}(\rho^*_{SE})$. This is the so-called mutual induced disturbance introduced by Luo [63]. Moreover if, following Refs. [76,77], we maximize $\mathcal{I}(\rho^*_{SE})$ over $\{\mathcal{P}^*_m, \mathcal{Q}^*_\mu\}$, then the inclusive entropy production is equal to the (symmetric) quantum discord [64,78] of the state ρ'_{SE}. On the other hand, the noninclusive entropy production in Eq. (15) is given by the total correlations in state ρ'_{SE}, that is, $\Delta_{\rm i} S = \Delta_{\rm i} S_{\rm inc} + \mathcal{I}(\rho^*_{SE}) = \mathcal{I}(\rho'_{SE})$, and it is independent of the choice of the local projectors of the final measurements $\{\mathcal{P}^*_m, \mathcal{Q}^*_\mu\}$.

The entropy production per trajectory $\Delta_{\rm i} s_\gamma$ can be calculated as explained in Sec. III. Recall that we may obtain both the inclusive and noninclusive entropy production depending on our choice for the initial state of the backward process, and that the two quantities verify the integral fluctuation theorem (26).

In Fig. 3, we show the probability distribution of the entropy production $P(\Delta_{\rm i} s_\gamma)$ for $\beta\epsilon = 2.5$ and $\alpha = 0.8$. Blue solid bars correspond to the noninclusive version, and purple dashed bars correspond to the inclusive one. The latter depends on the final measurements. Here, we have taken, as final projectors, the local energy eigenbasis, $\{\mathcal{P}^*_m = |m\rangle\langle m|_S, \mathcal{Q}^*_\mu = |\mu\rangle\langle\mu|_E\}$ for $m, \mu = 0, 1$. The different types of average entropy production are plotted

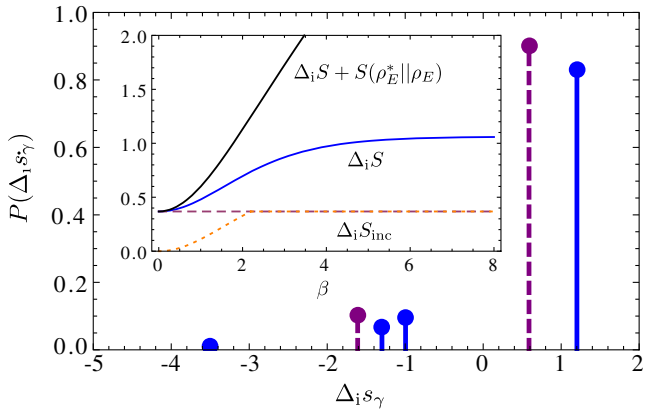

FIG. 3. Probability distribution $P(\Delta_{\rm i} s_\gamma)$ of the entropy production per trajectory for noninclusive (blue solid line) and inclusive (purple dashed line) cases. Initial states of the system and environment correspond to parameters $\alpha = 0.8$ and $\beta\epsilon = 2.5$. Inset: Plot of the different versions of the average entropy production as a function of β ($\epsilon = 1$ and $\alpha = 0.8$).

in the inset figure as functions of β for the same value of $\alpha = 0.8$. There, black and blue solid lines correspond to the average noninclusive entropy production with and without the term $S(\rho_E^*||\rho_E)$ due to local disturbance of the environment [see Eq. (29)], respectively. Dashed and dotted lines show the average inclusive entropy production for different choices of the local projectors in the final measurement $\{\mathcal{P}_m^*, \mathcal{Q}_\mu^*\}$. The purple dashed line is obtained when the final projectors are given by the local energy eigenbasis $\{\mathcal{P}_m^* = |m\rangle\langle m|_S, \mathcal{Q}_\mu^* = |\mu\rangle\langle\mu|_E\}$ for $m, \mu = 0, 1$. The orange dotted line is the symmetric quantum discord, obtained when maximizing $\mathcal{I}(\rho_{SE}^*)$.

As mentioned in Sec. II C, inclusive and noninclusive entropy production apply to different physical situations depending on how the system and the environment are manipulated after the process. If the system and environment are separated and every further manipulation is local, then we do not make use of the classical correlations given by the mutual information $\mathcal{I}(\rho_{SE}^*)$; in this case, the noninclusive entropy production is the magnitude that adequately describes the increase of entropy. On the other hand, global operations on the whole system + environment can make use of those correlations and, for instance, extract more energy from a thermal bath. We illustrate this possibility in our simple example by considering a second CNOT interaction after the final local measurements. For simplicity, we perform the final measurements in the local energy basis, $\{\mathcal{P}_m^* = |m\rangle\langle m|_S, \mathcal{Q}_\mu^* = |\mu\rangle\langle\mu|_E\}$ for $m, \mu = 0, 1$. Applying these projectors to state ρ'_{SE} in Eq. (82), one obtains the final global state

$$\rho_{SE}^* = \frac{1}{4}(\mathbb{I} + \kappa\sigma_z \otimes \sigma_z). \tag{83}$$

Applying the second CNOT to this state, one gets

$$\rho''_{SE} = U_{\text{CNOT}}\rho_{SE}^* U_{\text{CNOT}}^\dagger = \rho_S^* \otimes \rho_E, \tag{84}$$

where ρ_E is the initial thermal state of the environment. As we can see, in this second process, the system and environment become completely decorrelated after interaction, while a work $W_{\text{ext}} = \text{Tr}[(H_S + H_E)(\rho''_{SE} - \rho_{SE}^*)] = \epsilon(1/2 - e^{-\beta\epsilon}/Z_E)$ is extracted when performing the second gate. Notice that the extracted work equals the work performed in the first gate. This work extraction is impossible if we only have local operations at our disposal, for which the final state ρ_{SE}^* is completely equivalent to the uncorrelated state $\rho_S^* \otimes \rho_E^*$.

This simple example highlights the importance of distinguishing between inclusive and noninclusive entropy production in a small finite-size environment. Similar conclusions can be applied for the term $S(\rho_E^*||\rho_E)$.

B. Autonomous thermal machine

Consider an autonomous three-level thermal machine powered by three thermal reservoirs at different temperatures, as depicted in Fig. 4 [44,79–82]. Each bath mediates a different transition between the energy levels, $\{|g\rangle, |e_A\rangle, |e_B\rangle\}$. The Hamiltonian of the system is

$$H_S = \hbar\omega_1|e_A\rangle\langle e_A| + \hbar(\omega_1 + \omega_2)|e_B\rangle\langle e_B|; \tag{85}$$

that is, the three possible transitions $g \leftrightarrow e_A$, $e_A \leftrightarrow e_B$, and $g \leftrightarrow e_B$ have frequency gaps ω_1, ω_2, and $\omega_3 \equiv \omega_1 + \omega_2$, respectively. Each transition is weakly coupled to a bosonic thermal reservoir in equilibrium at inverse temperature $\beta_r = 1/kT_r$ with $r = 1, 2, 3$, where we assume $\beta_1 \geq \beta_3 \geq \beta_2$ for concreteness.

The dynamics of the three-level thermal machine can be described by a Lindblad master equation obtained in the weak coupling limit by standard techniques from open quantum systems theory [4,5,60]. It reads

$$\dot{\rho}_t = -\frac{i}{\hbar}[H_S, \rho_t] + \mathcal{L}_1(\rho_t) + \mathcal{L}_2(\rho_t) + \mathcal{L}_3(\rho_t), \tag{86}$$

where ρ_t is the density operator of the three-level system and Lamb-Stark shifts have been neglected. The three dissipative terms in the above equation describe the irreversible dynamical contributions induced by each of the three thermal reservoirs:

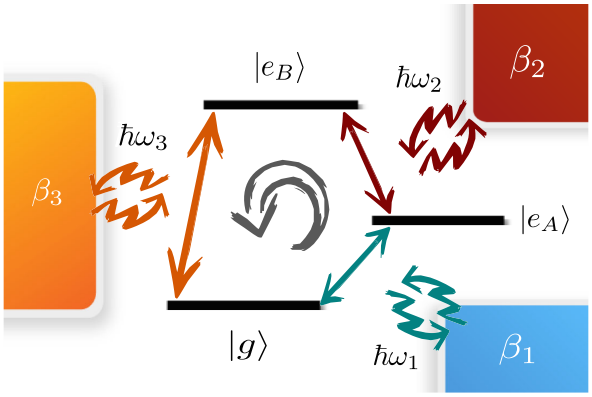

FIG. 4. Schematic diagram of a three-level thermal machine acting as a refrigerator. The three transitions of the machine are weakly coupled to thermal reservoirs at temperatures β_1, β_2, and β_3, inducing jumps between the machine energy levels (double arrows). In a refrigeration cycle, the machine performs a sequence of three jumps $|g\rangle \to |e_A\rangle \to |e_B\rangle \to |g\rangle$, where it absorbs a quantum of energy $\hbar\omega_1$ from the cold reservoir, together with a quantum $\hbar\omega_2$ from the hot one, while emitting a quantum $\hbar\omega_3$ into the reservoir at intermediate temperature.

$$\mathcal{L}_r(\rho_t) = \Gamma_{\downarrow}^{(r)}\left(a_r\rho_t a_r^\dagger - \frac{1}{2}\{a_r^\dagger a_r, \rho_t\}\right) + \Gamma_{\uparrow}^{(r)}\left(a_r^\dagger\rho_t a_r - \frac{1}{2}\{a_r a_r^\dagger, \rho_t\}\right), \quad (87)$$

$r = 1, 2, 3$, where $a_1 = |g\rangle\langle e_A|$, $a_2 = |e_A\rangle\langle e_B|$ and $a_3 = |g\rangle\langle e_B|$ are the ladder operators of the three-level system. Equation (87) describes the emission and absorption of excitations of energy $\hbar\omega_r$ to or from reservoir r, at rates $\Gamma_{\downarrow}^{(r)} = \gamma_r(n_r^{\rm th}+1)$ and $\Gamma_{\uparrow}^{(r)} = \gamma_r n_r^{\rm th}$, fulfilling detailed balance $\Gamma_{\downarrow}^{(r)} = e^{\beta_r\hbar\omega_r}\Gamma_{\uparrow}^{(r)}$. Here, $n_r^{\rm th} = (e^{\beta_r\hbar\omega_r}-1)^{-1}$ is the mean number of excitations of energy $\hbar\omega_r$ in reservoir r, and $\gamma_r \ll \omega_{r'}$ $\forall r, r' = 1, 2, 3$ are the spontaneous emission decay rates associated with each transition. The heat fluxes entering from the reservoirs associated with the imbalance in emission and absorption can be defined as $\dot{Q}_r = \mathrm{Tr}[H_S\mathcal{L}_r(\rho_t)]$ for $r = 1, 2, 3$, and the first law of thermodynamics reads $\dot{U} = \mathrm{Tr}[H_S\dot{\rho}_S] = \dot{Q}_1 + \dot{Q}_2 + \dot{Q}_3$.

Therefore, in our example, we have six Lindblad operators ($r = 1, 2, 3$),

$$L_{\downarrow}^{(r)} = \sqrt{\Gamma_{\downarrow}^{(r)}}a_r, \qquad L_{\uparrow}^{(r)} = \sqrt{\Gamma_{\uparrow}^{(r)}}a_r^\dagger, \quad (88)$$

that define the infinitesimal CPTP map (62) with the Kraus representation given by Eqs. (63) and (64). In particular,

$$M_{\downarrow}^{(r)} = \sqrt{dt}L_{\downarrow}^{(r)} = \sqrt{dt\Gamma_{\downarrow}^{(r)}}a_r, \quad (89)$$

$$M_{\uparrow}^{(r)} = \sqrt{dt}L_{\uparrow}^{(r)} = \sqrt{dt\Gamma_{\uparrow}^{(r)}}a_r^\dagger. \quad (90)$$

Here, the stochastic jumps during the evolution correspond to simple transitions between the energy levels $\{|g\rangle, |e_A\rangle, |e_B\rangle\}$. Therefore, the stochastic dynamics is completely equivalent to a classical Markov process if the initial state of the machine is diagonal in the Hamiltonian eigenbasis. In particular, the stationary state reads

$$\pi = \pi_g|g\rangle\langle g| + \pi_A|e_A\rangle\langle e_A| + \pi_B|e_B\rangle\langle e_B|. \quad (91)$$

In Appendix D, we explicitly calculate the occupation probabilities π_g, π_A, and π_B. Nevertheless, the transient dynamics could exhibit some quantum effects when the initial state exhibits coherences in the Hamiltonian eigenbasis. For instance, it has recently been pointed out that initial coherence can be used to reach lower temperatures during the transient dynamics [83,84].

The backward trajectory $\tilde{\gamma} = \{m, (k_N, t_N), \ldots, (k_1, t_1), n\}$ is defined by the inverse sequence of events with respect to γ, occurring in the backward process. We consider the initial state of the backward process as the inverted final state of the forward process, $\Theta_S\rho_{t_f}\Theta_S^\dagger$, while the thermal reservoirs have the same state as in the forward process. We further assume the simplest form for the time-inversion operator Θ_S, namely, the complex conjugation, i.e., $\Theta_S\psi = \psi^*$, which commutes with any matrix with real entries, as the Hamiltonian and the jump operators a_r, $a_r^\dagger$.

The Lindblad operators in this case come in pairs $L_{\downarrow}^{(r)} = e^{\beta_r\hbar\omega_r/2}L_{\uparrow}^{(r)\dagger}$. Hence, the stochastic entropy change in the environment σ_k^E for each operator L_k is given by Eq. (74), where the label k takes on the six possible values $k = (\uparrow, r)$ and $k = (\downarrow, r)$ with $r = 1, 2, 3$:

$$\sigma_{\downarrow}^{(r)} = \beta_r\hbar\omega_r, \qquad \sigma_{\uparrow}^{(r)} = -\beta_r\hbar\omega_r. \quad (92)$$

This is as expected since the upward jump r induced by the operator $L_{\downarrow}^{(r)}$ in the forward trajectory γ dissipates a heat $\hbar\omega_r$ to the reservoir at inverse temperature β_r. Equivalently, in the downward jump r, a heat $\hbar\omega_r$ is extracted from the thermal bath, reducing its entropy by an amount $\beta_r\hbar\omega_r$. The Kraus operators of the backward map are given by Eq. (75): $\tilde{M}_{\downarrow}^{(r)} = M_{\uparrow}^{(r)}$, $\tilde{M}_{\uparrow}^{(r)} = M_{\downarrow}^{(r)}$, and $\tilde{M}_0 = \Theta_S M_0\Theta_S^\dagger$ for the no-jump evolution. Indeed, by virtue of Eq. (72), we obtain $\tilde{U}_{\rm eff} = \Theta_S U_{\rm eff}^\dagger\Theta_S^\dagger = U_{\rm eff}$ for the effective evolution operator describing the dynamics between jumps in the backward process. From the above equations, we see that the backward map $\tilde{\mathcal{E}}$ is obtained from the forward map $\mathcal{E}$ inverting the jumps. We also notice that, consequently, the backward map $\tilde{\mathcal{E}}$ admits the time-reversed steady state $\tilde{\pi} = \Theta_S\pi\Theta_S^\dagger = \pi$ as an invariant state.

We next construct the dual and dual-reverse processes for the model. The condition for the Lindblad operators to be of the form in Eq. (38) is fulfilled here. Indeed, the nonequilibrium potential, $\Phi = -\ln\pi$, obeys $[\Phi, H_S] = 0$ and

$$[\Phi, L_k^{(r)}] = \Delta\phi_k^{(r)}L_k^{(r)}, \quad [\Phi, L_k^{(r)\dagger}] = -\Delta\phi_k^{(r)}L_k^{(r)\dagger}, \quad (93)$$

where the nonequilibrium potential changes associated with each jump in the trajectory read

$$\Delta\phi_0 = 0, \quad \Delta\phi_{r\downarrow} = -\beta_r'\hbar\omega_r, \quad \Delta\phi_{r\uparrow} = \beta_r'\hbar\omega_r. \quad (94)$$

Here, we have introduced the quantities $\beta_1' = \ln(\pi_0/\pi_1)/\hbar\omega_1$, $\beta_2' = \ln(\pi_1/\pi_2)/\hbar\omega_2$, and $\beta_3' = \ln(\pi_1/\pi_2)/\hbar\omega_3$, which can be seen as the local inverse temperature (or virtual temperature [85–87]) of each transition in the steady state π. As shown in Appendix D, they determine the direction of the heat flow in the stationary regime; i.e., if $\beta_r' > \beta_r$, then the temperature of reservoir r is higher than the local temperature of the machine and the heat $\dot{Q}_r$ is positive (energy flows from the reservoir to the machine), and vice versa. Moreover, for $\beta_r' \simeq \beta_r$, the heat flow is proportional to $\beta_r' - \beta_r$; therefore, the difference $\beta_r' - \beta_r$ can be considered as a thermodynamic force for the heat

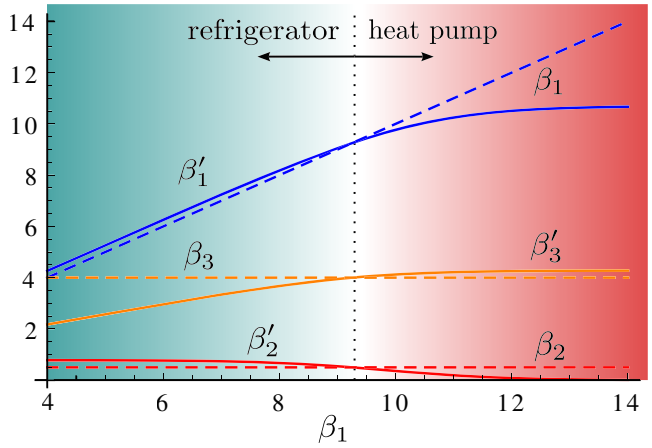

FIG. 5. Comparison between the inverse effective (or virtual) temperatures β_r' (solid lines) and the real inverse temperatures of the reservoirs β_r (dashed lines) for $r = 1, 2, 3$ (blue, red, orange), as a function of β_1 when $\hbar\omega_1 = 1$ and $\hbar\omega_2 = 1.5$. In the refrigerator regime, the transition $g \leftrightarrow e_A$ is, at an effective temperature, colder than the coldest reservoir, $\beta_1' \geq \beta_1$, inducing heat extraction from it, while the other transitions induce dissipation of heat to the reservoir at intermediate temperature, $\beta_2 \geq \beta_2'$, and absorption of heat in the hotter one, $\beta_2' \geq \beta_2$. In the heat pump regime, the three heat flows change directions as the previous inequalities become inverted.

flow between the reservoir r and the system. In Fig. 5, we plot the local inverse temperatures β_r' compared to the reservoir temperatures β_r for a specific choice of $\beta_2 = 0.5$ and $\beta_3 = 4$ and as a function of β_1, the inverse temperature of the coldest bath [we use units of $(\hbar\omega_1)^{-1}$]. There is a point, around $\beta_1 = 9.3$, where $\beta_r' = \beta_r$ and all the heat flows in the stationary regime vanish. Below that point, the steady heat flow from the coldest reservoir at inverse temperature β_1 is positive; i.e., the machine acts as a refrigerator that extracts energy from the coldest bath 1. On the other hand, for $\beta_1 > 9.3$, heat flows from the machine to the hottest bath at inverse temperature β_2, so the machine acts as a heat pump capable of heating up the hottest reservoir 2.

The Kraus operators for dual and dual-reverse maps, $\mathcal{D}$ and $\tilde{\mathcal{D}}$, can be obtained from Eqs. (46) and (41), respectively, by using Eqs. (92) and (94). They read

$$D_{\downarrow}^{(r)} = \sqrt{dt}e^{(\beta_r'-\beta_r)\hbar\omega_r}L_{\downarrow}^{(r)}, \tag{95}$$

$$D_{\uparrow}^{(r)} = \sqrt{dt}e^{-(\beta_r'-\beta_r)\hbar\omega_r}L_{\uparrow}^{(r)}, \tag{96}$$

$$\tilde{D}_{\downarrow}^{(r)} = \sqrt{dt}e^{-\beta_r'\hbar\omega_r}L_{\downarrow}^{(r)}, \tag{97}$$

$$\tilde{D}_{\uparrow}^{(r)} = \sqrt{dt}e^{\beta_r'\hbar\omega_r}L_{\uparrow}^{(r)}. \tag{98}$$

We see that the dual and dual-reversed dynamics induce similar jumps in the three-level system but with modified rates depending on the differences $\beta_r' - \beta_r$. Only when $\beta_r' = \beta_r$ for each r does the dual process become equal to the forward process, and hence the dual-reverse process equals the backward process (see Fig. 5).

Notice that Eq. (93), together with the backward map having $\tilde{\pi} = \pi$ as an invariant state, gives sufficient conditions to ensure the existence of the three fluctuation theorems for the adiabatic, nonadiabatic, and total entropy productions during trajectory γ. They explicitly read

$$\Delta_{\rm i}s_\gamma^{\rm a} = \sum_{r=1}^{3}(\beta_r' - \beta_r)q_\gamma^{(r)}, \tag{99}$$

$$\Delta_{\rm i}s_\gamma^{\rm na} = \sigma_{nm}^S - \sum_{r=1}^{3}\beta_r' q_\gamma^{(r)}, \tag{100}$$

$$\Delta_{\rm i}s_\gamma = \sigma_{nm}^S - \sum_{r=1}^{3}\beta_r q_\gamma^{(r)}, \tag{101}$$

where σ_{nm}^S is the stochastic entropy increase in the system, and $q_\gamma^{(r)} = \hbar\omega_r(n_\uparrow^{(r)} - n_\downarrow^{(r)})$ is the stochastic heat entering the system from reservoir r, with $n_{\uparrow\downarrow}^{(r)}$ being the total number of upward or downward jumps in transition r. The expression for the adiabatic entropy production is particularly interesting since it is equal to the entropy generated by the heat transfer between reservoirs at inverse temperatures β_r and β_r'. In particular, the adiabatic entropy production is identically zero when $\beta_r = \beta_r'$, even though it is possible to have transient flows of heat.

We can now calculate the average rates of nonequilibrium potential and reservoir entropy changes:

$$\langle\dot{\sigma}^{(r)}\rangle = \sum_{k=\uparrow,\downarrow}{\rm Tr}[L_k^{(r)\dagger}L_k^{(r)}\rho_t]\sigma_k^{(r)} = -\beta_r\dot{Q}_r, \tag{102}$$

$$\dot{\Phi}_r = \sum_{k=\uparrow,\downarrow}{\rm Tr}[L_k^{(r)\dagger}L_k^{(r)}\rho_t]\Delta\phi_k^{(r)} = \beta_r'\dot{Q}_r, \tag{103}$$

where we split into three parts the nonequilibrium potential flow $\dot{\Phi} = \dot{\Phi}_1 + \dot{\Phi}_2 + \dot{\Phi}_3 = -{\rm Tr}[\dot{\rho}_S \ln\pi]$. The entropy production rates hence read

$$\dot{S}_{\rm a} = \sum_r(\beta_r' - \beta_r)\dot{Q}_r \geq 0, \tag{104}$$

$$\dot{S}_{\rm na} = \dot{S} - \sum_r\beta_r'\dot{Q}_r \geq 0, \tag{105}$$

$$\dot{S}_{\rm i} = \dot{S} - \sum_r\beta_r\dot{Q}_r \geq 0, \tag{106}$$

showing the same structure as the trajectory entropies in Eqs. (99)–(101). Since there is no driving in this example,

the nonadiabatic entropy production reads as in Eq. (80), and it equals $\Delta S_{\rm na} = S(\rho_0||\pi)$ for a full relaxation to the steady state π.

In the steady state, we have $\dot{S}_{\rm na} = 0$, and the first law becomes $\sum_r \dot{Q}_r^{\rm ss} = 0$. This implies that the only contribution to the entropy production rate is the adiabatic one, which can be written as

$$\dot{S}_{\rm a} = \dot{S}_{\rm i} = (\beta_3 - \beta_2)\dot{Q}_2^{\rm ss} - (\beta_1 - \beta_3)\dot{Q}_1^{\rm ss} \geq 0. \tag{107}$$

This equation can be used to bound the efficiency of the machine in the different regimes of operation. For instance, the efficiency of the machine acting as a refrigerator is given by

$$\epsilon = \frac{\dot{Q}_1^{\rm ss}}{\dot{Q}_2^{\rm ss}} \leq \frac{\beta_3 - \beta_2}{\beta_1 - \beta_3} \equiv \epsilon_C, \tag{108}$$

where ϵ_C is the so-called Carnot efficiency of a refrigerator [85].

C. Periodically driven cavity mode

Our third example consists of a single electromagnetic field mode with frequency ω in a microwave cavity with slight losses in one of the two mirrors. The losses of the cavity are produced by the weak coupling of the cavity mode to a bosonic thermal reservoir in equilibrium at inverse temperature $\beta = 1/kT$. In addition, an external laser of the same frequency ω and weak intensity drives the cavity mode producing excitations. The Hamiltonian of the system can be expressed as $H_S(t) = H_0 + V_S(t)$ consisting of two terms: The first one is the Hamiltonian of the undriven mode $H_0 = \hbar\omega a^\dagger a$, and

$$V_S(t) = i\hbar(\epsilon a^\dagger e^{-i\omega t} - \epsilon^* a e^{i\omega t}) \tag{109}$$

describes the effect of the classical resonant laser field with complex amplitude $\epsilon = |\epsilon|e^{i\varphi}$. Here, the subscript S stands for the Schrödinger picture, whereas operators and density matrices without any subscript will correspond to the interaction picture with respect to H_0 (H_0 is, of course, the same in the two pictures). Figure 6 shows a schematic picture of the setup.

The reduced evolution of the cavity mode can be described by the following Lindblad master equation [60]:

$$\dot{\rho}_S(t) = -\frac{i}{\hbar}[H_S(t), \rho_S(t)] + \mathcal{L}(\rho_S(t)), \tag{110}$$

with the dissipative part

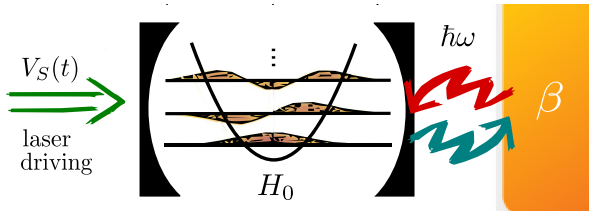

FIG. 6. Schematic picture of the setup. The intracavity mode H_0 is externally driven by a resonant laser field $V_S(t)$ while in weak contact with the environment at inverse temperature β, producing the emission and absorption of photons.

$$\mathcal{L}(\rho) = \Gamma_\downarrow\left(a\rho a^\dagger - \frac{1}{2}\{a^\dagger a, \rho\}\right) + \Gamma_\uparrow\left(a^\dagger \rho a - \frac{1}{2}\{aa^\dagger, \rho\}\right). \tag{111}$$

This term accounts for emission and absorption of photons by the cavity mode from the equilibrium reservoir at respective rates $\Gamma_\downarrow = \gamma_0(n^{\rm th} + 1)$ and $\Gamma_\uparrow = \gamma_0 n^{\rm th}$. Here, again, $n^{\rm th} = (e^{-\beta\hbar\omega} - 1)^{-1}$, and γ_0 is the spontaneous emission decay rate in the absence of driving. The dissipative term $\mathcal{L}(\rho)$ does not depend on the driving: It induces jumps in the eigenbasis of H_0 and is also invariant under the change of picture. Notice that this is an approximation. For slow driving, for instance, the bath induces jumps between the instantaneous eigenstates of the Hamiltonian $H_S(t)$. The dissipator (111) is valid for weak driving and weak coupling with the thermal bath, that is, $\gamma_0 \sim |\epsilon| \ll \omega$ [88].

In the interaction picture with respect to H_0, the Lindblad equation (110) reads [60]

$$\dot{\rho}(t) = -\frac{i}{\hbar}[V, \rho(t)] + \mathcal{L}(\rho(t)), \tag{112}$$

where $V = i\hbar(\epsilon a^\dagger - \epsilon^* a)$ is the driving Hamiltonian in the interaction picture, which turns out to be constant.

Before discussing the FT applied to this example, let us calculate the energetics of the system from the Lindblad equation. For this purpose, it is more convenient to express the internal energy in the Schrödinger picture: $U(t) = {\rm Tr}[H_S(t)\rho_S(t)]$. The first law reads $\dot{U}(t) = \dot{W}(t) + \dot{Q}(t)$, where the average work is given by

$$\begin{aligned}\dot{W}(t) &= {\rm Tr}[\dot{H}_S(t)\rho_S(t)] \\ &= \hbar\omega{\rm Tr}[(\epsilon a^\dagger e^{-i\omega t} + \epsilon^* a e^{i\omega t})\rho_S(t)] \\ &= \hbar\omega{\rm Tr}[(\epsilon a^\dagger + \epsilon^* a)\rho(t)].\end{aligned} \tag{113}$$

We denote the average energy change not accounted for by work as

$$\dot{Q}(t) = \mathrm{Tr}[H_S(t)\dot{\rho}_S(t)] = \mathrm{Tr}[H_S(t)\mathcal{L}(\rho_S(t))] = \mathrm{Tr}[(H_0 + V)\mathcal{L}(\rho(t))], \tag{114}$$

although it is not necessarily equal to the heat, i.e., the energy reversibly exchanged with a thermal reservoir that accounts for the reservoir's entropy change [89]. Below, we discuss in detail the physical nature of this energy transfer.

The steady state of the dynamics (112) obeys $-(i/\hbar)[V,\pi] + \mathcal{L}(\pi) = 0$. This equation can be solved by noticing that the term $[V,\rho]$ in Eq. (112) cancels under the transformation $a \to a - \alpha$, where $\alpha = 2\epsilon/\gamma_0$. The resulting steady state is

$$\pi = \mathcal{D}(\alpha)\frac{e^{-\beta H_0}}{Z_0}\mathcal{D}^\dagger(\alpha), \tag{115}$$

where $Z_0 = \mathrm{Tr}[\exp(-\beta H_0)]$, and $\mathcal{D}(\alpha) = \exp(\alpha a^\dagger - \alpha^* a)$ is the unitary displacement operator in optical phase space, fulfilling $\mathcal{D}(\alpha)a\mathcal{D}^\dagger(\alpha) = a - \alpha$, $\mathcal{D}^\dagger(\alpha) = \mathcal{D}(-\alpha)$. In contrast to the undriven case, here the cavity does not reach equilibrium with the reservoir: Coherences in the energy basis do not decay to zero because of the work performed by the external laser. Notice also that the state π defines a limit cycle (unitary orbit) in the Schrödinger picture. In the stationary regime, $\pi_S(t) = e^{-iH_0 t/\hbar}\pi e^{iH_0 t/\hbar}$; i.e., the mode rotates in optical phase space, according to the free evolution $\dot{\pi}_S = (-i/\hbar)[H_0, \pi_S]$.

The energetics in this stationary regime is rather simple. The internal energy is constant, even though the state $\pi_S(t)$ depends on time: $U_{\mathrm{ss}} = \mathrm{Tr}[H_S\pi_S] = \mathrm{Tr}[(H_0 + V)\pi] = \mathrm{Tr}[H_0\pi] = \hbar\omega(n^{\mathrm{th}} + |\alpha|^2)$, which is bigger than the thermal average energy $\hbar\omega n^{\mathrm{th}}$. The laser introduces energy at a rate

$$\dot{W}_{\mathrm{ss}} = \hbar\omega\mathrm{Tr}[(\epsilon a^\dagger + \epsilon^* a)\pi] = \hbar\omega\gamma_0|\alpha|^2 \geq 0, \tag{116}$$

which is dissipated to the thermal bath $\dot{Q}_{\mathrm{ss}} = -\dot{W}_{\mathrm{ss}}$.

The FT can be applied both to the Schrödinger and to the interaction picture. Here, it is is more convenient to determine the forward and backward processes in the interaction picture, where there is no driving. The Kraus operators for the map $\mathcal{E}$ in Eq. (62) read, in this case,

$$M_0 = \mathbb{I} - dt\left(\frac{i}{\hbar}V + \frac{1}{2}\sum_{k=\downarrow,\uparrow} L_k^\dagger L_k\right),$$

for the no-jump evolution, and

$$M_\downarrow = \sqrt{dt}L_\downarrow = \sqrt{dt\Gamma_\downarrow}a,$$
$$M_\uparrow = \sqrt{dt}L_\uparrow = \sqrt{dt\Gamma_\uparrow}a^\dagger,$$

for the downward and upward jumps corresponding to emission and absorption of photons.

The trajectory $\gamma = \{n, (k_1, t_1), \ldots, (k_N, t_N), m\}$ is then constructed as in the previous example by counting the jumps induced by the reservoir and registering the times at which they occur.

Since the forward dynamics is governed by a single pair of Lindblad operators $\{L_\downarrow = \sqrt{\Gamma_\downarrow}a, L_\uparrow = \sqrt{\Gamma_\uparrow}a^\dagger\}$, condition (70) allows us to obtain the stochastic entropy changes in the reservoir:

$$\sigma_0^E = 0, \qquad \sigma_\downarrow^E = \beta\hbar\omega, \qquad \sigma_\uparrow^E = -\beta\hbar\omega. \tag{117}$$

In other words, in a downward (upward) jump, the entropy in the environment increases (decreases) by $\beta\hbar\omega$, corresponding to a transfer of energy $\hbar\omega$. On average, this transfer of energy equals $\mathrm{Tr}[H_0\mathcal{L}(\rho(t))]$, whereas the energy not accounted for by work is given by Eq. (114), i.e., by $\dot{Q}(t) = \mathrm{Tr}[(H_0 + V)\mathcal{L}(\rho(t))]$. The origin of this discrepancy is the choice of a dissipator (111) independent of the driving. As already mentioned, the dissipator is valid for weak driving [88], when the term $\mathrm{Tr}[V\mathcal{L}(\rho(t))] \sim O(\gamma|\epsilon_0|)$ is negligible.

However, it is worth noticing that our approach does not depend on the physical nature of the environment and its interaction with the system. As shown in Sec. V, once a Lindblad equation like (110), with a given set of Lindblad operators for its unraveling, has been specified—no matter how it has been derived—it induces an entropy change in the environment given by Eq. (117). This is a direct consequence of the microreversibility that yields condition (70) on the Lindblad operators. When these operators come in pairs, as is the case in our example, the condition determines the entropy change in the environment [see Eq. (74)].

Therefore, if one could conceive physical situations where the Lindblad equation (110) is exact, then the entropy production would be given by Eq. (117) and the energy transfer $\mathrm{Tr}[V\mathcal{L}(\rho(t))]$ would not contribute to the entropy of the environment. A clue to the nature of this energy transfer is provided by Ref. [55]. In that paper, Elouard *et al.* introduce a driven two-level system in an engineered thermal bath where excitations occur through a third level with a very short lifetime and transitions are monitored by measuring emitted photons. The resulting Lindblad equation is the analog of Eq. (110) for a two-level system, and the entropy change in the environment is precisely Eq. (117). These results show that the energy transfer $\mathrm{Tr}[V\mathcal{L}(\rho(t))]$ is due to the collapse of a coherent state induced by the photon detection. This energy transfer does not change the entropy of the universe and has been categorized either as "measurement work" [31,74] or as "quantum heat" [54,55] due to measurement.

The Kraus operators of the backward map are given by Eq. (75):

$$\tilde{M}_0 = \Theta M_0 \Theta^\dagger = M_0, \tag{118}$$

$$\tilde{M}_\downarrow = \sqrt{dt}\tilde{L}_\downarrow = \sqrt{dt}\Theta L_\uparrow \Theta^\dagger = M_\uparrow, \tag{119}$$

$$\tilde{M}_\uparrow = \sqrt{dt}\tilde{L}_\uparrow = \sqrt{dt}\Theta L_\downarrow \Theta^\dagger = M_\downarrow, \tag{120}$$

implying again that the forward and the backward maps are equivalent; i.e., the jumps up (down) in the forward process are transformed in jumps down (up) in the backward process.

The main feature of this example is that the key condition (38) is not fulfilled. Recall that this condition is needed to define the dual and dual-reverse dynamics as well as the stochastic adiabatic and nonadiabatic entropy production at the trajectory level. Using the expression for the stationary state, Eq. (115), we can calculate the nonequilibrium potential in the interaction picture,

$$\begin{aligned}\Phi &= -\ln \pi = \beta \mathcal{D}(\alpha) H_0 \mathcal{D}^\dagger(\alpha) + \ln Z_0 \\ &= \beta H_0 - \beta\hbar\omega|\alpha|(x_\varphi - |\alpha|) + \ln Z_0,\end{aligned} \tag{121}$$

where we have introduced the field quadrature

$$x_\varphi = a^\dagger e^{i\varphi} + a\ e^{-i\varphi}. \tag{122}$$

The nonequilibrium potential Φ in Eq. (121) does not obey Eq. (73) because the Lindblad operators appearing in the dynamics (112) promote jumps among the eigenstates of the unperturbed Hamiltonian H_0, instead of the eigenstates of the steady density matrix π. This implies that we cannot associate a single change in the nonequilibrium potential with each of the Lindblad jump operators, nor to M_0. As a consequence, the entropy production per trajectory cannot be decomposed in adiabatic and nonadiabatic contributions, and the corresponding fluctuation theorems do not apply. However, the conditions in Eq. (73) can be recovered in some cases by properly including the effect of the driving on the Lindblad operators [74].

Even though the adiabatic and nonadiabatic entropy production cannot be defined at the trajectory level, we can calculate their averages [75] using, for instance, Eq. (78):

$$\dot{S}_{\rm na} = \dot{S} - \beta(\dot{U} - \hbar\omega|\alpha|\dot{X}_\varphi), \tag{123}$$

$$\dot{S}_{\rm a} = \dot{S}_{\rm i} - \dot{S}_{\rm na} = \beta(\dot{W} - \hbar\omega|\alpha|\dot{X}_\varphi). \tag{124}$$

Here, we have used $\dot{S}_{\rm i} = \dot{S} - \beta\dot{Q}$ and $\dot{U}(t) = \langle \dot{H}_0 \rangle = \dot{Q} + \dot{W}$, and introduced $\dot{X}_\varphi \equiv {\rm Tr}[x_\varphi \dot{\rho}(t)]$, the rate at which the cavity field mode is displaced by the laser (with phase φ) until the steady state is reached. Since there are no fluctuation theorems for these quantities, in principle, they could be negative. The nonadiabatic entropy production, however, still obeys Eq. (79) and, since the steady state π is constant in the interaction picture, it can be written as the change of the relative entropy between the state $\rho(t)$ and π, which is always positive: $\dot{S}_{\rm na} = -\dot{S}(\rho(t)||\pi) \geq 0$. This is not the case of the adiabatic entropy production $\dot{S}_{\rm a}$, which indeed can take on negative values. The expression for $\dot{S}_{\rm a}$ in Eq. (123) equals the entropy production in the steady state, $\dot{S}_{\rm a} \to \beta W_{\rm ss} = -\beta Q_{\rm ss} \geq 0$. However, it can be negative in the transient regime, as shown in Fig. 7 (see also Appendix E). In Fig. 7(a), we depict the evolution of the three entropy production rates when the cavity mode starts in a Gibbs thermal state in equilibrium with the reservoir temperature, $\rho_0 = \exp(-\beta H_0)/Z_0$. We find that the entropy of the mode is kept constant during the evolution, $\dot{S} = 0\ \forall t$, which implies $\dot{S}_{\rm i} = -\beta\dot{Q} \geq 0$ and $\dot{S}_{\rm na} = \beta(\hbar\omega|\alpha|\dot{X}_\varphi - \dot{U}) \geq 0$. On the other hand, the adiabatic entropy production rate $\dot{S}_{\rm a} = \beta(\dot{W} - \mu\dot{X}_\varphi)$ is negative

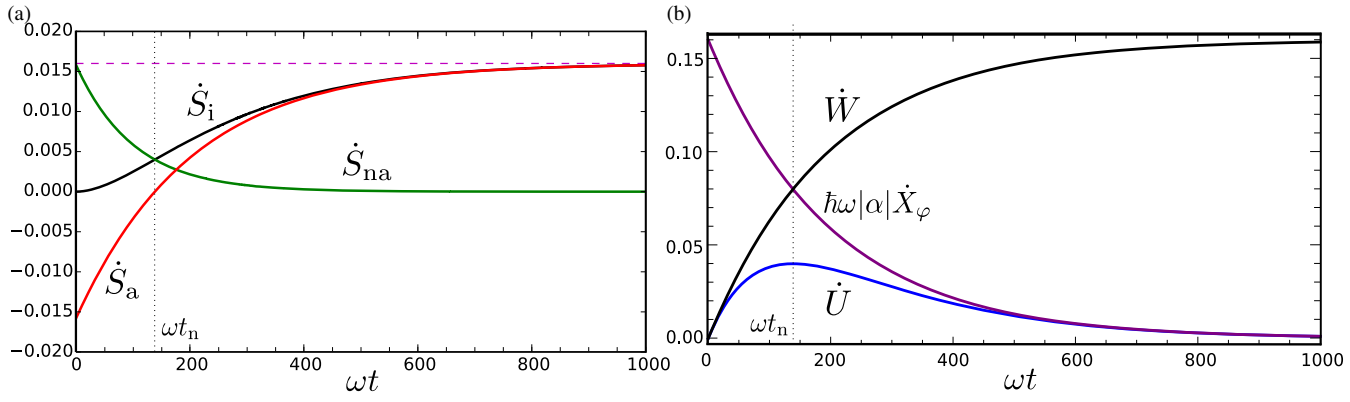

FIG. 7. Time evolution of (a) adiabatic ($\dot{S}_{\rm a}$), nonadiabatic ($\dot{S}_{\rm na}$), and total ($\dot{S}_{\rm i}$) entropy production rates represented by solid lines, and (b) input power ($\dot{W}$), rate at which the cavity mode absorbs energy ($\dot{U}$), and displacement rate ($\dot{X}_\varphi$). The cavity mode starts in equilibrium with the thermal reservoir, $\rho_0 = e^{-\beta\hat{H}_0}Z$, and the laser driving is switched on at $t = 0$. The dashed line in (a) corresponds to $\beta\dot{W}_{\rm ss}$, and we use vertical dotted lines to highlight the instant of time at which the adiabatic entropy production rate changes its sign (t_n). We use parameters $\epsilon = 0.02\omega$, $\gamma_0 = 0.01\omega$, and temperature $kT = 10\hbar\omega$, for $\hbar\omega = 1$ units.

for times $t < t_n \equiv 2\ln 2/\gamma_0$. It is worth mentioning that for this initial condition, the term $\mathrm{Tr}[V\mathcal{L}(\rho(t))]$ in the energetics vanishes at any time t.

To explore the origin of this purely quantum effect, we plot the energetics of the relaxation process in Fig. 7(b). The cavity mode absorbs energy at constant entropy from the external laser until the periodic steady state is reached, $\dot{U} = \dot{W}e^{-\gamma_0 t/2}$, where $\dot{W} = \dot{W}_{\mathrm{ss}}(1 - e^{-\gamma_0 t/2}) \geq 0$ is the input power and, consequently, heat is dissipated at a rate $-\dot{Q} = \dot{W}(1 - e^{-\gamma_0 t/2}) \geq 0$. When the relaxation is completed, the input laser power is fully dissipated into the reservoir, i.e., $\dot{Q}_{\mathrm{ss}} = -\dot{W}_{\mathrm{ss}}$. The energy absorbed by the cavity mode during the evolution is fully employed to generate the unitary displacement α, that is, $\Delta U = \hbar\omega|\alpha|\Delta X_\varphi = \hbar\omega|\alpha|^2$. However, the transient dynamics ruling this process is far from trivial. The cavity mode is always displaced, i.e., gaining coherence, at a higher rate than energy, $\dot{U} = \hbar\omega|\alpha|\dot{X}_{\mathcal{S}}(1 - e^{-\gamma_0 t/2})$, in accordance with the positive nonadiabatic entropy production rate. In addition, by comparing Figs. 7(a) and 7(b), the energetic meaning of the adiabatic entropy production rate can be clarified. In the initial transient where $\dot{S}_{\mathrm{a}} < 0$, the coherence gain surpasses the input power, i.e., $\hbar\omega|\alpha|\dot{X}_\varphi > \dot{W}$, which in turn implies that the rate at which the cavity mode gains energy speeds up in this period, $\ddot{U} > 0$. At time t_n, when $\dot{S}_{\mathrm{a}} = 0$, we have $\dot{W} = \hbar\omega|\alpha|\dot{X}_\varphi = \dot{W}_{\mathrm{ss}}/2$, and $\dot{U}$ peaks at its maximum. After this time, the adiabatic entropy production rate is positive $\dot{S}_{\mathrm{a}} > 0$, implying $\hbar\omega|\alpha|\dot{X}_\varphi < \dot{W}$, and $\dot{U}$ decreases until it becomes zero in the long time run, when the periodic steady state is reached. In conclusion, we obtain that the sign of the adiabatic entropy production rate spotlights the acceleration in the internal energy changes of the cavity mode.

VII. CONCLUSIONS

In this paper, we have analyzed the production of entropy in general processes embedded in a two-measurement protocol, with local measurements performed in both the system and the environment. Our first main result is the fluctuation theorem (23), which compares the probability of forward and backward trajectories. Particularizing this expression to certain initial conditions of the backward process, one can obtain FT's for the change of inclusive (14) and exclusive (15) entropy production, i.e., for the entropy production that results from keeping or neglecting the classical correlations generated between the system and the environment during the process. These differences have been illustrated for the case of two qubits interacting through a CNOT quantum gate.

We have also explored whether it is possible to split the total entropy production into adiabatic and nonadiabatic contributions, as it is customary in classical systems far from equilibrium [22,23]. For that purpose, we have introduced a dual dynamics for the reduced evolution of the system, which in turn allowed us to clarify the interpretation of previous FT's derived for quantum CPTP maps [33]. We have shown that the aforementioned decomposition is possible only if the reduced dynamics satisfies a certain condition, namely, Eq. (38). In fact, we give an explicit example where that condition is not fulfilled and the adiabatic entropy production takes on negative values. This is a pure quantum feature whose consequences, we believe, are worth further exploring.

Our results can be applied to a broad range of quantum processes including multipartite environments and concatenations of CPTP maps. In particular, we developed, in detail, the application to processes described by Lindblad master equations. We have introduced a general method to identify the environmental entropy change during the trajectories induced by quantum jumps [see Eq. (70) and below], which allows us to recover the FT's. The meaning of the adiabatic and nonadiabatic terms becomes clear in this situation since the nonadiabatic contribution tends to zero for quasistatic driving.

Finally, we have studied the decomposition of the total entropy production in two specific situations of interest: an autonomous three-level thermal machine and a dissipative cavity mode resonantly driven by a classical field.

Summarizing, our results provide an exhaustive characterization of the entropy production in open quantum systems undergoing arbitrary processes. This includes systems in contact with nonthermal or finite-size reservoirs, configurations with several equilibrium baths with different temperatures or chemical potentials, driven systems, etc. In all those cases, one should be able to assess the entropy production and characterize its fluctuations within the theoretical framework presented in this paper. Therefore, our results clarify the origin of entropy production from coarse graining and its link to thermodynamical notions when particular choices for the environment are made.

ACKNOWLEDGMENTS

We thank Gili Bisker for comments. The authors acknowledge funding from Ministerio de Economía y Competitividad (MINECO) (Proyectos TerMic, FIS2014-52486-R and CONTRACT, FIS2017-83709-R). G. M. acknowledges support from FPI Grant No. BES-2012-054025. This work has been partially supported by COST Action MP1209 "Thermodynamics in the Quantum Regime."

APPENDIX A: INFINITESIMAL CHANGES IN THE STATE OF THE RESERVOIR

In this appendix, we show that the term $S(\rho_E^*||\rho_E)$ appearing in Eq. (29) is negligible for infinitesimal changes in the environment density matrix. Let us assume the change in the environment density operator in the following general form:

$$\rho_E^* = \rho_E + \epsilon\Delta\rho_E, \tag{A1}$$

where $\mathrm{Tr}[\Delta\rho_E] = 0$ and $\epsilon \geq 0$ is a small real number. Using the definition of the quantum relative entropy, we can then write

$$S(\rho_E^*||\rho_E) = S(\rho_E) - S(\rho_E^*) - \epsilon\mathrm{Tr}[\Delta\rho_E \ln \rho_E]. \tag{A2}$$

In the following, we show that if $\epsilon \ll 1$, then $S(\rho_E^*) - S(\rho_E) \simeq -\epsilon\mathrm{Tr}[\Delta\rho_E \ln \rho_E]$, and consequently, $S(\rho_E^*||\rho_E) \to 0$. This can be done by applying perturbation theory. Let the eigenvalues and eigenstates of ρ_E^*, the set $\{q_\mu^*, |\phi_\mu^*\rangle\}$, be expanded to second order in ϵ:

$$q_\mu^* \simeq q_\mu + \epsilon q_\mu^{(1)} + \epsilon^2 q_\mu^{(2)}, \tag{A3}$$

$$|\phi_\mu^*\rangle \simeq |\phi_\mu\rangle + \epsilon|\phi_\mu^{(1)}\rangle + \epsilon^2|\phi_\mu^{(2)}\rangle, \tag{A4}$$

where the zeroth-order contributions obey $\rho_E|\phi_\mu\rangle = q_\mu|\phi_\mu\rangle$, and we have, for the first-order terms,

$$q_\mu^{(1)} = \langle\phi_\mu|\Delta\rho|\phi_\mu\rangle, \tag{A5}$$

$$|\phi_\mu^{(1)}\rangle = \sum_{\nu\neq\mu} \frac{\langle\phi_\nu|\Delta\rho|\phi_\mu\rangle}{q_\mu - q_\nu}|\phi_\nu\rangle. \tag{A6}$$

We now calculate the entropy change up to second order in ϵ:

$$\begin{aligned} S(\rho_E^*) - S(\rho_E) &= -\sum_\mu q_\mu^* \ln q_\mu^* + \sum_\nu q_\nu \ln q_\nu \\ &\simeq -\epsilon\sum_\mu q_\mu^{(1)} \ln q_\mu \\ &\quad - \epsilon^2\left(q_\mu^{(2)} \ln q_\mu + \sum_\mu \frac{q_\mu^{(1)\,2}}{2q_\mu}\right), \end{aligned} \tag{A7}$$

to be compared with

$$\begin{aligned} -\epsilon\mathrm{Tr}[\Delta\rho_E \ln \rho_E] &= -\epsilon\sum_\mu \langle\phi_\mu|\Delta\rho|\phi_\mu\rangle \ln q_\mu \\ &= -\epsilon\sum_\mu q_\mu^{(1)} \ln q_\mu. \end{aligned} \tag{A8}$$

The above equations (A7) and (A8) are equal up to first order, differing in $\mathcal{O}(\epsilon^2)$. Therefore, using Eq. (A2), we conclude that

$$S(\rho_E^*||\rho_E) \simeq -\epsilon^2\left(q_\mu^{(2)} \ln q_\mu + \sum_\mu \frac{q_\mu^{(1)2}}{2q_\mu}\right) = \mathcal{O}(\epsilon^2), \tag{A9}$$

and when $\epsilon \ll 1$, we can consider $S(\rho_E^*||\rho_E) \to 0$ up to first order, in contrast to the change in entropy [Eq. (A7)].

APPENDIX B: MULTIPARTITE ENVIRONMENTS

Recall that we assume R ancillary systems in an uncorrelated state, $\rho_E = \rho_1 \otimes \ldots \otimes \rho_R$, and local measurements in each separate environmental ancilla. We denote the local density operators of the environmental ancilla r at the beginning and at the end of the (forward) process as

$$\rho_r = \sum_\nu q_\nu^{(r)} \mathcal{Q}_\nu^{(r)}, \qquad \rho_r^* = \sum_\mu q_\mu^{(r)*} \mathcal{Q}_\mu^{(r)*}, \tag{B1}$$

with eigenvalues $q_\nu^{(r)}$ and $q_\mu^{(r)*}$, and orthogonal projectors onto its eigenstates $\mathcal{Q}_\nu^{(r)} = |\chi_\nu^{(r)}\rangle\langle\chi_\nu^{(r)}|_E$ and $\mathcal{Q}_\mu^{(r)*} = |\chi_\mu^{(r)*}\rangle\langle\chi_\mu^{(r)*}|_E$.

The generalization of the results is then straightforward by considering the same steps and assumptions as before. The reduced system dynamics is again given by Eq. (7), but the operators $M_{\mu\nu}$ now use collective indices

$$(\mu, \nu) = \{(\nu^{(1)}, \mu^{(1)}), \ldots, (\nu^{(R)}, \mu^{(R)})\}, \tag{B2}$$

representing the set of transitions obtained in the projective measurements of all environmental ancillas:

$$|\chi_{\nu^{(r)}}^{(r)}\rangle_E \to |\chi_{\mu^{(r)}}^{(r)*}\rangle_E \quad \text{for } r = 1, \ldots, R. \tag{B3}$$

In other words, the Kraus operators of the forward process are given by

$$M_{\mu\nu} = \left(\prod_{r=1}^R \sqrt{q_{\nu^{(r)}}^{(r)}}\right) \langle\chi_{\mu^{(1)}}^{(1)*} \cdots \chi_{\mu^{(R)}}^{(R)*}|_E U_\Lambda |\chi_{\nu^{(1)}}^{(1)} \cdots \chi_{\nu^{(R)}}^{(R)}\rangle_E, \tag{B4}$$

and analogously for the Kraus operators of the backward process (31), we have

$$\begin{aligned} \tilde{M}_{\nu\mu} = &\left(\prod_{r=1}^R \sqrt{\tilde{q}_{\mu^{(r)}}^{(r)}}\right) \\ &\times \langle\chi_{\nu^{(1)}}^{(1)} \cdots \chi_{\nu^{(R)}}^{(R)}|_E \Theta_E^\dagger U_{\tilde{\Lambda}} \Theta_E |\chi_{\mu^{(1)}}^{(1)*} \cdots \chi_{\mu^{(R)}}^{(R)*}\rangle_E. \end{aligned} \tag{B5}$$

The key relation (32) necessary to obtain the fluctuation theorem for the total entropy production (23) hence follows as well in this case, with a decomposition of the environment boundary term

$$\sigma_{\mu\nu}^E = \sum_{r=1}^R \sigma_{\mu^{(r)}\nu^{(r)}}^{(r)} \tag{B6}$$

being $\sigma_{\mu^{(r)}\nu^{(r)}}^{(r)} \equiv -\ln \tilde{q}_{\mu^{(r)}}^{(r)} + \ln q_{\nu^{(r)}}^{(r)}$.

The application of the above formalism introducing the dual and dual-reverse processes follows immediately in the

same manner, leading to the fluctuation theorems for the adiabatic and nonadiabatic entropy production in detailed and integral versions, Eqs. (42), (48), and (49). The adiabatic entropy production per trajectory and its average then read, in this case,

$$\Delta_{\rm i} s^{\rm a}_{\mu\nu} = \sum_{r=1}^{R} \sigma^{r}_{\mu^{(r)}\nu^{(r)}} + \Delta\phi_{\mu\nu}, \tag{B7}$$

$$\Delta_{\rm i} S_{\rm a} = \sum_{r=1}^{R} S(\rho_r^*) - S(\rho_r) + \langle \Delta\phi \rangle \geq 0, \tag{B8}$$

where in the averaged version we again set (uncorrelated) reversible boundaries, $\tilde{\rho}_{SE} = \Theta(\rho_S^* \otimes \rho_1^* \otimes \ldots \otimes \rho_R^*)\Theta^\dagger$.

APPENDIX C: CONCATENATIONS OF CPTP MAPS

In the following, we focus on the derivation of FT's for concatenations of CPTP maps reported in Sec. IV E. Here, we assume the environment is a single reservoir or ancilla. However, the extension to multiple reservoirs follows in the same manner as in the one-map case (see Appendix B).

Consider the map concatenation Ω in Eq. (57). For any map $\mathcal{E}^{(l)}$ in the sequence, the environmental ancilla starts in a generic state

$$\rho_E^{(l)} \equiv \sum_\alpha q_\alpha^{(l)} \mathcal{Q}_\alpha^{(l)}, \tag{C1}$$

and it is measured at the beginning and at the end of the interaction with the system, generating outcomes labeled as ν_l and μ_l, respectively. The measurements are specified by the rank-one projective operators $\{\mathcal{Q}_{\nu_k}^{(l)}\} \equiv \{|\phi_{\nu_l}^{(l)}\rangle\langle\phi_{\nu_l}^{(l)}|\}$ for the initial measurement and $\{\mathcal{Q}_{\mu_l}^{(l)*} \equiv |\phi_{\mu_l}^{(l)*}\rangle\langle\phi_{\mu_l}^{(l)*}|\}$ for the final one. Under these conditions, each map in the concatenation can be written as

$$\mathcal{E}^{(l)}(\cdot) = \sum_{\mu_l,\nu_l} M^{(l)}_{\mu_l,\nu_l}(\cdot) M^{(l)\dagger}_{\mu_l\nu_l}, \tag{C2}$$

with $M^{(l)}_{\mu_l\nu_l} \equiv \sqrt{q_{\nu_l}^{(l)}}\langle\phi_{\mu_l}^{(l)*}|U_\Lambda^{(l)}|\phi_{\nu_l}^{(l)}\rangle$, where the unitary evolution $U_\Lambda^{(l)}$ is as in Eq. (2). Here, we always consider the same total time-dependent Hamiltonian $H(t)$, following an arbitrary driving protocol $\Lambda = \{\lambda_t | 0 \leq t \leq N\tau\}$. For convenience, the latter can also be split into N intervals; hence, the partial protocol $\Lambda_l = \{\lambda_t | t_{l-1} \leq t \leq t_l\}$ generates the unitary operator $U_\Lambda^{(l)}$.

A quantum trajectory in this context is defined as follows. At time $t = 0$, we start with our system in ρ_S, which is measured with eigenprojectors $\{\mathcal{P}_n\}$, obtaining outcome n. Then, the sequence of maps Ω defined in Eq. (57) is applied, obtaining outcomes $\{\mu_l, \nu_l\}$ from each of the $l = 1, \ldots, N$ pairs of measurements in the environment. Finally, at time $t = N\tau$, the system is measured again with arbitrary (rank-one) projectors $\{\mathcal{P}_m^*\}$, giving outcome m. A quantum trajectory is now completely specified by the set of outcomes, $\gamma = \{n, (\nu_1, \mu_1), \ldots, (\nu_N, \mu_N), m\}$, and it occurs with probability

$$P(\gamma) = p_n \mathrm{Tr}[\mathcal{P}_m^* \mathcal{E}^{(N)}_{\mu_N\nu_N} \circ \ldots \circ \mathcal{E}^{(1)}_{\mu_1\nu_1}(\mathcal{P}_n)]. \tag{C3}$$

Now, we can apply the same arguments in the previous sections to construct the three different processes used to state the FT's. For the initial state of the backward process, we consider again an arbitrary initial state of the system $\tilde{\rho}_S = \sum_m \tilde{p}_m \Theta \mathcal{P}_m^* \Theta^\dagger$, uncorrelated from the environment initial states $\tilde{\rho}_E^{(l)} = \sum_\alpha \tilde{q}_\alpha \Theta \mathcal{Q}_\alpha^* \Theta^\dagger$, and apply the sequence of maps $\tilde{\Omega} = \tilde{\mathcal{E}}^{(1)} \circ \ldots \circ \tilde{\mathcal{E}}^{(l)} \circ \ldots \circ \tilde{\mathcal{E}}^{(N)}$, generating a trajectory $\tilde{\gamma} = \{m, (\mu_1, \nu_1), \ldots, (\mu_N, \nu_N), n\}$ with probability

$$\tilde{P}(\tilde{\gamma}) = \tilde{p}_m \mathrm{Tr}[\Theta_S \mathcal{P}_n \Theta_S^\dagger \tilde{\mathcal{E}}^{(1)}_{\nu_1\mu_1} \circ \ldots \circ \tilde{\mathcal{E}}^{(N)}_{\nu_N\mu_N}(\Theta_S \mathcal{P}_m^* \Theta_S^\dagger)]. \tag{C4}$$

Here, the backward maps $\tilde{\mathcal{E}}^{(l)}$ and their corresponding operations are defined by each map $\mathcal{E}^{(l)}$ in the concatenation Ω by applying Eqs. (30) and (31).

Dual and dual-reverse maps and operations also follow from the definitions in Sec. IV when conditions (38) and $\tilde{\mathcal{E}}^{(l)}(\tilde{\pi}^{(l)}) = \tilde{\pi}^{(l)}$ are met for each map in the sequence. The corresponding probabilities for trajectory γ in the dual process and trajectory $\tilde{\gamma}$ in the dual-reverse process are

$$P_D(\gamma) = p_n \mathrm{Tr}[\mathcal{P}_m^* \mathcal{D}^{(N)}_{\mu_N\nu_N} \circ \ldots \circ \mathcal{D}^{(1)}_{\mu_1\nu_1}(\mathcal{P}_n)], \tag{C5}$$

$$\tilde{P}_D(\tilde{\gamma}) = \tilde{p}_m \mathrm{Tr}[\Theta \mathcal{P}_n \Theta^\dagger \tilde{\mathcal{D}}^{(1)}_{\nu_1,\mu_1} \circ \ldots \circ \tilde{\mathcal{D}}^{(N)}_{\nu_N\mu_N}(\Theta \mathcal{P}_m^* \Theta^\dagger)], \tag{C6}$$

where in the dual-reverse trajectories we again took the sequence of maps in inverted order; that is, we applied $\tilde{\mathcal{D}}^{(1)} \circ \ldots \circ \tilde{\mathcal{D}}^{(N)}$ over the initial state $\tilde{\rho}_S$.

Again, the Kraus operators for the backward, dual, and dual-reverse trajectories fulfill the set of operator detailed-balance relations:

$$\Theta^\dagger \tilde{M}^{(l)}_{\nu\mu} \Theta = e^{-\sigma^E_{\mu_l,\nu_l}/2} M^{(l)\dagger}_{\mu\nu}, \tag{C7}$$

$$\Theta^\dagger \tilde{D}^{(l)}_{\nu\mu} \Theta = e^{\Delta\phi^{(l)}_{\mu\nu}/2} M^{(l)\dagger}_{\mu\nu}, \tag{C8}$$

$$D^{(l)}_{\mu\nu} = e^{-(\sigma^E_{\mu_l,\nu_l} + \Delta\phi^{(l)}_{\mu\nu})/2} M^{(l)}_{\mu\nu}, \tag{C9}$$

where the nonequilibrium potential changes are defined with respect to the invariant state $\pi^{(l)}$ of each map $\mathcal{E}^{(l)}$ as in the single map case: $\Delta\phi^{(l)}_{\mu\nu} = -\ln \pi^{(l)}_\mu + \ln \pi^{(l)}_\nu$.

The set of Eqs. (C7)–(C9) immediately implies the detailed FT's for concatenations in Eqs. (58)–(60). Its

corresponding integral versions and second-law-like inequalities follow immediately as a corollary.

Finally, it is interesting to consider the expression of the average nonequilibrium potential change during the whole sequence. By denoting $\rho_S(t_l)$ the reduced state of the system at time t_l, we have

$$\Delta\Phi = \sum_{l=1}^{N} \mathrm{Tr}[\mathcal{E}^{(l)}_{\mu_l\nu_l}(\rho_S(t_{l-1}))]\Delta\phi^{(l)}_{\mu_l\nu_l} = \sum_{l=1}^{N} \mathrm{Tr}[(\rho_S(t_l) - \rho_S(t_{l-1}))\Phi_l], \tag{C10}$$

where $\Phi_l = -\ln \pi^{(l)}$. The above expression can be decomposed into the following boundary and path contributions:

$$\Delta\Phi_b = \mathrm{Tr}[\rho'_S\Phi_N] - \mathrm{Tr}[\rho_S\Phi_1], \tag{C11}$$

$$\Delta\Phi_p = -\sum_{l=1}^{N-1} \mathrm{Tr}[\rho_S(t_l)(\Phi_{l+1} - \Phi_l)]. \tag{C12}$$

When all the maps in the concatenation have the same invariant state, $\Phi_{l+1} = \Phi_l \equiv \Phi \forall l$, we obtain $\Delta\Phi_p = 0$, while $\Delta\Phi_b = \mathrm{Tr}[(\rho'_S - \rho_S)\Phi]$ and we recover the expression for the single map case, cf. Eq. (53). On the other hand, the boundary term only vanishes for cyclic processes, such that $\rho'_S = \rho_S$, implemented by cyclic concatenations with $\Phi_N = \Phi_1$. In this case, $\Delta\Phi_b = 0$, while $\Delta\Phi_p$ gives, in general, a nonzero contribution.

The dynamical versions of these boundary and path terms read

$$\dot{\Phi}_b = \frac{d}{dt}(\mathrm{Tr}[\rho_t\Phi(\lambda_t)]), \qquad \dot{\Phi}_p = -\mathrm{Tr}[\rho_t\dot{\Phi}(\lambda_t)], \tag{C13}$$

which are also analogous to their classical counterparts [21–23].

APPENDIX D: AUTONOMOUS QUANTUM THERMAL MACHINE DETAILS

The setup presented in Sec. VI constitutes the simplest model of an ideal quantum absorption heat pump and refrigerator, usually considered to operate at steady-state conditions [44,81,82]. We now focus on the heat pump configuration, but similar conclusions follow as well in the heat pump mode of operation. The cooling mechanism exploits the average heat flow entering from the reservoir at the hottest temperature, $\dot{Q}_2 > 0$, to continuously extract heat from the reservoir at the lowest temperature, $\dot{Q}_1 > 0$, while draining $\dot{Q}_3 < 0$ to the reservoir at the intermediate (inverse) temperature, β_3 (see Fig. 4).

The three average heat fluxes entering from the reservoirs associated with the imbalance in emission and absorption processes, $\dot{Q}_r = \mathrm{Tr}[H_S\mathcal{L}_r(\rho_t)]$, read

$$\dot{Q}_1 = \hbar\omega_1(\Gamma^{(1)}_{\uparrow}p_g(t) - \Gamma^{(1)}_{\downarrow}p_A(t)), \tag{D1}$$

$$\dot{Q}_2 = \hbar\omega_2(\Gamma^{(2)}_{\uparrow}p_A(t) - \Gamma^{(2)}_{\downarrow}p_B(t)), \tag{D2}$$

$$\dot{Q}_3 = \hbar\omega_3(\Gamma^{(3)}_{\uparrow}p_g(t) - \Gamma^{(3)}_{\downarrow}p_B(t)), \tag{D3}$$

where $p_i(t)$ are the instantaneous populations of the machine energy levels $|g\rangle$, $|e_A\rangle$, $|e_B\rangle$, and $\sum_i p_i(t) = 1$. The first law of thermodynamics in the model follows from the master equation (86):

$$\dot{U} = \mathrm{Tr}[H_S\dot{\rho}_S] = \dot{Q}_1 + \dot{Q}_2 + \dot{Q}_3, \tag{D4}$$

which, in the steady-state conditions, reads $\dot{Q}_1 + \dot{Q}_2 + \dot{Q}_3 = 0$. In such a case, the heat fluxes become

$$\dot{Q}_1 = \hbar\omega_1\Gamma^{(1)}_{\uparrow}\pi_g(1 - e^{-(\beta'_1-\beta_1)\hbar\omega_1}), \tag{D5}$$

$$\dot{Q}_2 = \hbar\omega_2\Gamma^{(2)}_{\uparrow}\pi_A(1 - e^{-(\beta'_2-\beta_2)\hbar\omega_2}), \tag{D6}$$

$$\dot{Q}_3 = \hbar\omega_3\Gamma^{(3)}_{\uparrow}\pi_g(1 - e^{-(\beta'_3-\beta_3)\hbar\omega_3}), \tag{D7}$$

where we employ the detailed balance relations $\Gamma^{(r)}_{\uparrow} = e^{\beta_r\hbar\omega_r}\Gamma^{(r)}_{\downarrow}$ and the definitions for the effective temperatures β'_r, for $r = 1, 2, 3$. Therefore, since the prefactors in all three above expressions are always positive, the direction of the heat fluxes is determined by the sign of the respective thermodynamic force $X_r \equiv \beta'_r - \beta_r$. Indeed, near equilibrium when $X_r \ll 1$, we may expand, to first order, the exponentials in Eqs. (D5)–(D7) and recover the well-known result of linear irreversible thermodynamics,

$$\dot{Q}_r = \alpha_r X_r, \tag{D8}$$

where α_r is a positive constant; that is, fluxes are proportional to thermodynamic forces. In any case, Eqs. (D5)–(D7) show that heat flows from the environment to a system transition, $\dot{Q}_r \geq 0$, if the latter is at an effective temperature lower than the former, $\beta'_r \geq \beta_r$.

The steady state of the dynamics [Eq. (91)], for the simpler case in which $\gamma_1 = \gamma_2 = \gamma_3 \equiv \gamma$, reads

$$\pi_g = \frac{e^{\beta_3\hbar\omega_3}(2e^{\beta_1\hbar\omega_1+\beta_2\hbar\omega_2} - 1) - e^{\beta_1\hbar\omega_1+\beta_2\hbar\omega_2}}{Z_\pi}, \tag{D9}$$

$$\pi_A = \frac{e^{\beta_2\hbar\omega_2}(e^{\beta_1\hbar\omega_1} - 2) + e^{\beta_3\hbar\omega_3}(2e^{\beta_2\hbar\omega_2} - 1)}{Z_\pi}, \tag{D10}$$

$$\pi_B = \frac{e^{\beta_3\hbar\omega_3} + e^{\beta_1\hbar\omega_1+\beta_2\hbar\omega_2} - 2}{Z_\pi}, \tag{D11}$$

where we define $Z_\pi \equiv e^{\beta_2\hbar\omega_2}(-2 + e^{\beta_1\hbar\omega_1}) - 2 + e^{\beta_3\hbar\omega_3}(2e^{\beta_2\hbar\omega_2}(1 + e^{\beta_1\hbar\omega_1}) - 1)$.

At steady-state conditions, the fridge or heat pump modes of operation can be obtained by properly tuning the energy-level spacings. Inserting the steady-state values in the expressions for the heat fluxes, we obtain

$$\dot{Q}_1^{\rm ss} = \gamma\hbar\omega_1\Delta/Z_\pi \geq 0, \quad \dot{Q}_2^{\rm ss} = \gamma\hbar\omega_2\Delta/Z_\pi \geq 0, \tag{D12}$$

and $\dot{Q}_3^{\rm ss} = -(\dot{Q}_1^{\rm ss} + \dot{Q}_2^{\rm ss}) \leq 0$, where $Z_\pi \geq 0$ and the quantity $\Delta \equiv (e^{\beta_3\hbar\omega_3} - e^{\beta_1\hbar\omega_1+\beta_2\hbar\omega_2}) \geq 0$. Therefore, for a fridge, we need $\Delta \geq 0$. This is guaranteed when the following design condition is met:

$$\omega_2 \geq \left(\frac{\beta_1 - \beta_3}{\beta_3 - \beta_2}\right)\omega_1. \tag{D13}$$

Notice also that when the above inequality is inverted, we obtain $\Delta \leq 0$, and the three heat flows invert its signs, hence generating the heat pump mode of operation.

APPENDIX E: TRANSIENT NEGATIVITY OF THE ADIABATIC ENTROPY PRODUCTION RATE

In this appendix, we provide further details on the dynamical evolution of thermodynamic quantities used in the description of the driving cavity model in Sec. VI C. In particular, we give explicit expressions for key quantities $\dot{X}_\varphi$, $\dot{W}$, and $\dot{Q}$, and discuss the adiabatic entropy production rate $\dot{S}_{\rm a}$, showing its transient negativity.

The explicit time evolution of the quantities $\dot{X}_\varphi$, $\dot{W}$, and $\dot{Q}$ can be obtained from the master equation (112). In order to do that, we first obtain the following equations for the evolution of the quantities $A \equiv a - \alpha$ and $A^\dagger A = a^\dagger a - |\alpha|(x_\varphi - |\alpha|)$. They read

$$\frac{d}{dt}\langle A\rangle_t = -\frac{\gamma_0}{2}\langle A\rangle_t, \tag{E1}$$

$$\frac{d}{dt}\langle A^\dagger A\rangle_t = -\gamma_0(\langle A^\dagger A\rangle_t - \langle A^\dagger A\rangle_\infty), \tag{E2}$$

where $\langle A^\dagger A\rangle_\infty = {\rm Tr}[A^\dagger A\pi] = {\rm Tr}[a^\dagger a(e^{-\beta H_0}/Z_0)] = n^{\rm th}$. Consequently, we obtain, as a result,

$$\langle A\rangle_t = \langle A\rangle_0 e^{-\gamma_0 t/2}, \tag{E3}$$

$$\langle A^\dagger A\rangle_t = \langle A^\dagger A\rangle_0 e^{-\gamma_0 t} + n^{\rm th}(1 - e^{-\gamma_0 t}). \tag{E4}$$

The transient evolution of the field quadrature $\langle x_\varphi\rangle_t \equiv {\rm Tr}[x_\varphi\rho_t]$ is then easily obtained from the above equations,

$$\dot{X}_\varphi = -\frac{\gamma_0}{2}(\langle x_\varphi\rangle_t - \langle x_\varphi\rangle_\infty). \tag{E5}$$

This means that $\langle x_\varphi\rangle_t$ exponentially converges to its steady-state value $\langle x_\alpha\rangle_\infty = 2|\alpha|$. Therefore, $\dot{X}_\varphi$ will be either positive or negative during the evolution, depending on the displacement of the initial state. If $\langle x_\varphi\rangle_0 \leq \langle x_\varphi\rangle_\infty$, then $\dot{X}_\varphi \geq 0\ \forall t$, and the system state increases its coherence in the energy basis; however, if $\langle x_\varphi\rangle_0 \geq \langle x_\varphi\rangle_\infty$, we have $\dot{X}_\varphi \leq 0\ \forall t$, and the coherence decreases. From Eq. (E5), we have

$$\langle x_\varphi\rangle_t = \langle x_\varphi\rangle_0 e^{-\gamma_0 t/2} + \langle x_\varphi\rangle_\infty(1 - e^{-\gamma_0 t/2}). \tag{E6}$$

Furthermore, we can now calculate the transient input power as

$$\begin{aligned}\dot{W} &= \hbar\omega{\rm Tr}[(\epsilon a^\dagger + \epsilon^* a)\rho_t] = \epsilon\langle a^\dagger\rangle_t + \epsilon^*\langle a\rangle_t \\ &= |\epsilon|\langle x_\varphi\rangle_0 + \dot{W}_{\rm ss}(1 - e^{-\gamma_0 t/2}),\end{aligned} \tag{E7}$$

where we use $\langle a\rangle_t = \langle A\rangle_t + \alpha$ together with Eq. (E3), and we recall that $\dot{W}_{\rm ss} = \hbar\omega|\alpha|^2$. Analogously, having Eq. (E4), the heat flow follows from

$$\begin{aligned}\dot{Q} &= {\rm Tr}[H_0\mathcal{L}(\rho_t)] = -\gamma_0(\langle a^\dagger a\rangle_t - n^{\rm th}) \\ &= -\gamma_0\hbar\omega(|\alpha|^2(1 - e^{-\gamma_0 t/2})^2 + |\alpha|\langle x_\varphi\rangle_0(1 - e^{-\gamma_0 t/2})e^{-\gamma_0 t/2} \\ &\quad + (\langle a^\dagger a\rangle_0 - n^{\rm th})),\end{aligned} \tag{E8}$$

where, in the last equality, we also use Eq. (E6). Notice that, for the initial state $\rho_0 = \exp(-\beta H_0)/Z_0$, we have $\langle a\rangle_0 = 0$ and $\langle a^\dagger a\rangle_0 = n^{\rm th}$, and then, using Eqs. (E7) and (E8), we obtain, for this case,

$$\dot{Q} = -\dot{W}(1 - e^{-\gamma_0 t/2}), \quad \dot{U} = \dot{W} + \dot{Q} = \dot{W}e^{-\gamma_0 t/2}. \tag{E9}$$

Finally, the adiabatic entropy production rate has been defined in Eq. (123):

$$\dot{S}_{\rm a} = \dot{S}_{\rm i} - \dot{S}_{\rm na} = \beta(\dot{W} - \hbar\omega|\alpha|\dot{X}_\varphi). \tag{E10}$$

We can obtain an explicit expression for its evolution by noticing that the following equality holds:

$$\dot{W} + \hbar\omega|\alpha|\dot{X}_\varphi = \dot{W}_{\rm ss}. \tag{E11}$$

Introducing this relation into Eq. (E10), we obtain

$$\dot{S}_a = \beta\dot{W}_{\rm ss} + \beta\hbar\omega|\alpha|\gamma_0(\langle x_\varphi\rangle - \langle x_\varphi\rangle_\infty). \tag{E12}$$

Notice now that Eq. (E12) is negative for any initial transient for which $\hbar\omega|\alpha|\dot{X}_\varphi < \hbar\omega|\alpha|\langle x_\varphi\rangle_\infty + \dot{W}_{\rm ss}/\gamma_0$. In particular, if the dynamics starts in any state diagonal in the H_0 basis, this happens for $t < t_n \equiv 2\ln(2)/\gamma_0$ as shown in Fig. 7 of Sec. VI C.

[1] U. Seifert, *Entropy Production along a Stochastic Trajectory and an Integral Fluctuation Theorem*, Phys. Rev. Lett. **95**, 040602 (2005).

[2] U. Seifert, *Stochastic Thermodynamics, Fluctuation Theorems and Molecular Machines*, Rep. Prog. Phys. **75**, 126001 (2012).

[3] C. Jarzynski, *Equalities and Inequalities: Irreversibility and the Second Law of Thermodynamics at the Nanoscale*, Annu. Rev. Condens. Matter Phys. **2**, 329 (2011).

[4] H.-P. Breuer and F. Petruccione, *The Theory of Open Quantum Systems* (Oxford University Press, Oxford, 2002).

[5] A. Rivas and S. F. Huelga, *Open Quantum Systems: An Introduction* (Springer, Berlin, Heidelberg, 2012).

[6] M. Campisi, P. Hänggi, and P. Talkner, *Colloquium: Quantum Fluctuation Relations: Foundations and Applications*, Rev. Mod. Phys. **83**, 771 (2011).

[7] M. Esposito, U. Harbola, and S. Mukamel, *Nonequilibrium Fluctuations, Fluctuation Theorems, and Counting Statistics in Quantum Systems*, Rev. Mod. Phys. **81**, 1665 (2009).

[8] S. Deffner and E. Lutz, *Nonequilibrium Entropy Production for Open Quantum Systems*, Phys. Rev. Lett. **107**, 140404 (2011).

[9] P. Gaspard, *Multivariate Fluctuation Relations for Currents*, New J. Phys. **15**, 115014 (2013).

[10] G. Watanabe, B. P. Venkatesh, P. Talkner, M. Campisi, and P. Hänggi, *Quantum Fluctuation Theorems and Generalized Measurements During the Force Protocol*, Phys. Rev. E **89**, 032114 (2014).

[11] G. B. Cuetara, M. Esposito, and A. Imparato, *Exact Fluctuation Theorem without Ensemble Quantities*, Phys. Rev. E **89**, 052119 (2014).

[12] R. Dorner, S. R. Clark, L. Heaney, R. Fazio, J. Goold, and V. Vedral, *Extracting Quantum Work Statistics and Fluctuation Theorems by Single-Qubit Interferometry*, Phys. Rev. Lett. **110**, 230601 (2013).

[13] L. Mazzola, G. De Chiara, and M. Paternostro, *Measuring the Characteristic Function of the Work Distribution*, Phys. Rev. Lett. **110**, 230602 (2013).

[14] M. Campisi, R. Blattmann, S. Kohler, D. Zueco, and P. Hänggi, *Employing Circuit QED to Measure Nonequilibrium Work Fluctuations*, New J. Phys. **15**, 105028 (2013).

[15] J. Goold, U. Poschinger, and K. Modi, *Measuring the Heat Exchange of a Quantum Process*, Phys. Rev. E **90**, 020101(R) (2014).

[16] A. J. Roncaglia, F. Cerisola, and J. P. Paz, *Work Measurement as a Generalized Quantum Measurement*, Phys. Rev. Lett. **113**, 250601 (2014).

[17] G. De Chiara, A. J. Roncaglia, and J. P. Paz, *Measuring Work and Heat in Ultracold Quantum Gases*, New J. Phys. **17**, 035004 (2015).

[18] T. B. Batalhão, A. M. Souza, L. Mazzola, R. Auccaise, R. S. Sarthour, I. S. Oliveira, J. Goold, G. De Chiara, M. Paternostro, and R. M. Serra, *Experimental Reconstruction of Work Distribution and Study of Fluctuation Relations in a Closed Quantum System*, Phys. Rev. Lett. **113**, 140601 (2014).

[19] S. An, J.-N. Zhang, M. Um, D. Lv, Y. Lu, J. Zhang, Z.-Q. Yin, H. T. Quan, and K. Kim, *Experimental Test of the Quantum Jarzynski Equality with a Trapped-Ion System*, Nat. Phys. **11**, 193 (2015).

[20] T. Hatano and S.-I. Sasa, *Steady-State Thermodynamics of Langevin Systems*, Phys. Rev. Lett. **86**, 3463 (2001).

[21] M. Esposito and C. Van den Broeck, *Three Detailed Fluctuation Theorems*, Phys. Rev. Lett. **104**, 090601 (2010).

[22] M. Esposito and C. Van den Broeck, *Three Faces of the Second Law. I. Master Equation Formulation*, Phys. Rev. E **82**, 011143 (2010).

[23] C. Van den Broeck and M. Esposito, *Three Faces of the Second Law. II. Fokker-Planck Formulation*, Phys. Rev. E **82**, 011144 (2010).

[24] G. Bisker, M. Polettini, T. R. Gingrich, and J. M. Horowitz, *Hierarchical Bounds on Entropy Production Inferred from Partial Information*, J. Stat. Mech. (2017) 093210.

[25] V. Vedral, *An Information-Theoretic Equality Implying the Jarzynski Relation*, J. Phys. A **45**, 272001 (2012).

[26] D. Kafri and S. Deffner, *Holevo's Bound from a General Quantum Fluctuation Theorem*, Phys. Rev. A **86**, 044302 (2012).

[27] R. Chetritie and K. Mallick, *Quantum Fluctuation Relations for the Lindblad Master Equation*, J. Stat. Phys. **148**, 480 (2012).

[28] T. Albash, D. A. Lidar, M. Marvian, and P. Zanardi, *Fluctuation Theorems for Quantum Processes*, Phys. Rev. E **88**, 032146 (2013).

[29] A. E. Rastegin and K. Życzkowski, *Jarzynski Equality for Quantum Stochastic Maps*, Phys. Rev. E **89**, 012127 (2014).

[30] S. Deffner, *Quantum Entropy Production in Phase Space*, Europhys. Lett. **103**, 30001 (2013).

[31] J. M. Horowitz and J. M. R. Parrondo, *Entropy Production along Nonequilibrium Quantum Jump Trajectories*, New J. Phys. **15**, 085028 (2013).

[32] K. Funo, Y. Watanabe, and M. Ueda, *Integral Quantum Fluctuation Theorems under Measurement and Feedback Control*, Phys. Rev. E **88**, 052121 (2013).

[33] G. Manzano, J. M. Horowitz, and J. M. R. Parrondo, *Nonequilibrium Potential and Fluctuation Theorems for Quantum Maps*, Phys. Rev. E **92**, 032129 (2015).

[34] Á. M. Alhambra, L. Masanes, J. Oppenheim, and C. Perry, *Fluctuating Work: From Quantum Thermodynamical Identities to a Second Law Equality*, Phys. Rev. X **6**, 041017 (2016).

[35] J. J. Park, S. W. Kim, and V. Vedral, *Fluctuation Theorem for Arbitrary Quantum Bipartite Systems*, arXiv:1705.01750.

[36] J. P. Pekola, P. Solinas, A. Shnirman, and D. V. Averin, *Calorimetric Measurement of Work in a Quantum System*, New J. Phys. **15**, 115006 (2013).

[37] S. Gasparinetti, K. L. Viisanen, O.-P. Saira, T. Faivre, M. Arzeo, M. Meschke, and J. P. Pekola, *Fast Electron Thermometry for Ultrasensitive Calorimetric Detection*, Phys. Rev. Applied **3**, 014007 (2015).
[38] S. Suomela, A. Kutvonen, and T. Ala-Nissila, *Quantum Jump Model for a System with a Finite-Size Environment*, Phys. Rev. E **93**, 062106 (2016).
[39] M. O. Scully, M. S. Zubairy, G. S. Agarwal, and H. Walther, *Extracting Work from a Single Heat Bath via Vanishing Quantum Coherence*, Science **299**, 862 (2003).
[40] A. Ü. C. Hardal and Ö. E. Müstecaplıoğlu, *Superradiant Quantum Heat Engine*, Sci. Rep. **5**, 12953 (2015).
[41] E. Lutz and R. Dillenschneider, *Energetics of Quantum Correlations*, Europhys. Lett. **88**, 50003 (2009).
[42] X. L. Huang, T. Wang, and X. X. Yi, *Effects of Reservoir Squeezing on Quantum Systems and Work Extraction*, Phys. Rev. E **86**, 051105 (2012).
[43] J. Roßnagel, O. Abah, F. Schmidt-Kaler, K. Singer, and Eric Lutz, *Nanoscale Heat Engine beyond the Carnot Limit*, Phys. Rev. Lett. **112**, 030602 (2014).
[44] L. A. Correa, J. P. Palao, D. Alonso, and G. Adesso, *Quantum-Enhanced Absorption Refrigerators*, Sci. Rep. **4**, 3949 (2014).
[45] G. Manzano, F. Galve, R. Zambrini, and J. M. R. Parrondo, *Entropy Production and Thermodynamic Power of the Squeezed Thermal Reservoir*, Phys. Rev. E **93**, 052120 (2016).
[46] J. Klaers, S. Faelt, A. Imamoglu, and E. Togan, *Squeezed Thermal Reservoirs as a Resource for a Nanomechanical Engine beyond the Carnot Limit*, Phys. Rev. X **7**, 031044 (2017).
[47] W. Niedenzu, D. Gelbwaser-Klimovsky, A. G. Kofman, and G. Kurizki, *On the Operation of Machines Powered by Quantum Non-thermal Baths*, New J. Phys. **18**, 083012 (2016).
[48] D. Reeb and M. M. Wolf, *An Improved Landauer Principle with Finite-Size Corrections*, New J. Phys. **16**, 103011 (2014).
[49] J. Goold, M. Paternostro, and K. Modi, *Nonequilibrium Quantum Landauer Principle*, Phys. Rev. Lett. **114**, 060602 (2015).
[50] M. Esposito, K. Lindenberg, and C. Van den Broeck, *Entropy Production as Correlation between System and Reservoir*, New J. Phys. **12**, 013013 (2010).
[51] T. Sagawa, *Second Law-like Inequalitites with Quantum Relative Entropy: An Introduction*, in *Lectures on Quantum Computing, Thermodynamics and Statistical Physics*, Kinki University Series on Quantum Computing, Vol. 8, edited by M. Nakahara (World Scientific, New Jersey, 2013).
[52] J. M. Horowitz and T. Sagawa, *Equivalent Definitions of the Quantum Nonadiabatic Entropy Production*, J. Stat. Phys. **156**, 55 (2014).
[53] B. Leggio, A. Napoli, A. Messina, and H. P. Breuer, *Entropy Production and Information Fluctuations along Quantum Trajectories*, Phys. Rev. A **88**, 042111 (2013).
[54] C. Elouard, D. A. Herrera-Martí, M. Clusel, and A. Auffèves, *The Role of Quantum Measurement in Stochastic Thermodynamics*, npj Quantum Information **3**, 9 (2017).
[55] C. Elouard, N. K. Bernardes, A. R. R. Carvalho, M. F. Santos, and A. Auffèves, *Probing Quantum Fluctuation Theorems in Engineered Reservoirs*, New J. Phys. **19**, 103011 (2017).
[56] J. P. Santos, G. T. Landi, and M. Paternostro, *Wigner Entropy Production Rate*, Phys. Rev. Lett. **118**, 220601 (2017).
[57] M. N. Bera, A. Riera, M. Lewestein, and A. Winter, *Thermodynamics as a Consequence of Information Conservation*, arXiv:1707.01750.
[58] B. Groisman, S. Popescu, and A. Winter, *Quantum, Classical, and Total Amount of Correlations in a Quantum State*, Phys. Rev. A **72**, 032317 (2005).
[59] K. Kraus, A. Böhm, J. D. Dollard, and W. H. Wootters, *States, Effects, and Operations: Fundamental Notions of Quantum Theory*, Lecture Notes in Physics (Springer-Verlag, Berlin, 1983).
[60] H. M. Wiseman and G. J. Milburn, *Quantum Measurement and Control* (Cambridge University Press, Cambridge, England, 2010).
[61] J. M. R. Parrondo, J. M. Horowitz, and T. Sagawa, *Thermodynamics of Information*, Nat. Phys. **11**, 131 (2015).
[62] M. A. Nielsen and I. L. Chuang, *Quantum Computation and Quantum Information* (Cambridge University Press, Cambridge, England, 2000).
[63] S. Luo, *Using Measurement-Induced Disturbance to Characterize Correlations as Classical or Quantum*, Phys. Rev. A **77**, 022301 (2008).
[64] K. Modi, A. Brodutch, H. Cable, T. Paterek, and V. Vedral, *The Classical-Quantum Boundary for Correlations: Discord and Related Measures*, Rev. Mod. Phys. **84**, 1655 (2012).
[65] M. H. Partovi, *Entanglement versus Stosszahlansatz: Disappearance of the Thermodynamic Arrow in a High-Correlation Environment*, Phys. Rev. E **77**, 021110 (2008).
[66] D. Jennings and T. Rudolph, *Entanglement and the Thermodynamic Arrow of Time*, Phys. Rev. E **81**, 061130 (2010).
[67] F. Haake, *Quantum Signatures of Chaos*, Springer Series in Synergetics, 3rd ed. (Springer, Berlin, 2010).
[68] D. Andrieux and P. Gaspard, *Quantum Work Relations and Response Theory*, Phys. Rev. Lett. **100**, 230404 (2008).
[69] T. Sagawa and M. Ueda, *Role of Mutual Information in Entropy Production under Information Exchanges*, New J. Phys. **15**, 125012 (2013).
[70] G. E. Crooks, *Quantum Operation Time Reversal*, Phys. Rev. A **77**, 034101 (2008).
[71] F. Fagnola and V. Umanità, *Generators of Detailed Balance Quantum Markov Semigroups*, Infin. Dimensional Anal. Quantum Probab. Relat. Top. **10**, 335 (2007).
[72] G. Lindblad, *On the Generators of Quantum Dynamical Semigroups*, Commun. Math. Phys. **48**, 119 (1976).
[73] K. Szczygielski, D. Gelbwaser-Klimovsky, and R. Alicki, *Markovian Master Equation and Thermodynamics of a Two-Level System in a Strong Laser Field*, Phys. Rev. E **87**, 012120 (2013).
[74] J. M. Horowitz, *Quantum-Trajectory Approach to the Stochastic Thermodynamics of a Forced Harmonic Oscillator*, Phys. Rev. E **85**, 031110 (2012).
[75] H. Spohn, *Entropy Production for Quantum Dynamical Semigroups*, J. Math. Phys. (N.Y.) **19**, 1227 (1978).
[76] S. Wu, U. V. Poulsen, and K. Mølmer, *Correlations in Local Measurements on a Quantum State, and Complementarity*

as an Explanation of Nonclassicality, Phys. Rev. A **80**, 032319 (2009).

[77] D. Girolami, M. Paternostro, and G. Adesso, *Faithful Nonclassicality Indicators and Extremal Quantum Correlations in Two-Qubit States*, J. Phys. A **44**, 352002 (2011).

[78] H. Ollivier and W. H. Zurek, *Quantum Discord: A Measure of the Quantumness of Correlations*, Phys. Rev. Lett. **88**, 017901 (2001).

[79] H. E. D. Scovil and E. O. Schulz-DuBois, *Three-Level Masers as Heat Engines*, Phys. Rev. Lett. **2**, 262 (1959).

[80] J. E. Geusic, E. O. Schulz-DuBois, and H. E. D. Scovil, *Quantum Equivalent of the Carnot Cycle*, Phys. Rev. **156**, 343 (1967).

[81] J. P. Palao, R. Kosloff, and J. M. Gordon, *Quantum Thermodynamic Cooling Cycle*, Phys. Rev. E **64**, 056130 (2001).

[82] R. Kosloff and A. Levy, *Quantum Heat Engines and Refrigerators: Continuous Devices*, Annu. Rev. Phys. Chem. **65**, 365 (2014).

[83] M. T. Mitchison, M. P. Woods, J. Prior, and M. Huber, *Coherence-Assisted Single-Shot Cooling by Quantum Absorption Refrigerators*, New J. Phys. **17**, 115013 (2015).

[84] J. B. Brask and N. Brunner, *Small Quantum Absorption Refrigerator in the Transient Regime: Time Scales, Enhanced Cooling, and Entanglement*, Phys. Rev. E **92**, 062101 (2015).

[85] N. Brunner, N. Linden, S. Popescu, and P. Skrzypczyk, *Virtual Qubits, Virtual Temperatures, and the Foundations of Thermodynamics*, Phys. Rev. E **85**, 051117 (2012).

[86] P. Skrzypczyk, R. Silva, and N. Brunner, *Passivity, Complete Passivity, and Virtual Temperatures*, Phys. Rev. E **91**, 052133 (2015).

[87] R. Silva, G. Manzano, P. Skrzypczyk, and N. Brunner, *Performance of Autonomous Quantum Thermal Machines: Hilbert Space Dimension as a Thermodynamical Resource*, Phys. Rev. E **94**, 032120 (2016).

[88] A. Rivas, A. D. K. Plato, S. F. Huelga, and M. B. Plenio, *Markovian Master Equations: A Critical Study*, New J. Phys. **12**, 113032 (2010).

[89] J. M. Horowitz and M. Esposito, *Work Producing Reservoirs: Stochastic Thermodynamics with Generalized Gibbs Ensembles*, Phys. Rev. E **94**, 020102(R) (2016).